



Article

Concentration-Dependent Pleiotropic Effects of Thymosin Beta4 and Cofilin on the Migratory Activity of Carcinoma Cells

Abdulatif Al Haj ¹, Kamila Ćwikłowska ², Antonina Joanna Mazur ^{1,†}, Beate Brand-Saberi ¹, Ewald Hannappel ³ and Hans Georg Mannherz ^{1,4,5,*}

- ¹ Department of Anatomy and Molecular Embryology, Ruhr-University, D-44780 Bochum, Germany; abdulatif.alhaj@rub.de (A.A.H.); antonina.mazur@uwr.edu.pl (A.J.M.); beate.brand-saberi@rub.de (B.B.-S.)
² Department of Cell Pathology, Faculty of Biotechnology, University of Wrocław, PL-50-383 Wrocław, Poland; kamilacwiklowska@gmail.com
³ Institute of Biochemistry, University of Erlangen, D-91054 Erlangen, Germany; ewald.hannappel@fau.de
⁴ Department of Cellular and Translational Physiology, Ruhr-University, D-44780 Bochum, Germany
⁵ Molecular and Experimental Cardiology, Institute for Research and Education, St. Josef Hospital, Clinics of the Ruhr-University, D-44780 Bochum, Germany
* Correspondence: hans.g.mannherz@rub.de; Tel.: +49-234-322-4553; Fax: +49-234-321-4474
† Current address: Department of Cell Pathology, Faculty of Biotechnology, University of Wrocław, PL-50-383 Wrocław, Poland.

Abstract: Background/Objectives: Tumor cell migration depends on the actin cytoskeleton modified by actin-binding proteins (ABPs). Overexpression of cofilin or thymosin beta4 (Tβ4) has been correlated with an increase or decrease in their migratory activity, respectively. Methods: Immunostaining of tumor cells and transfection with EGFP-tagged cofilin or bicistronic vectors leading to independent expression of EGFP and Tβ4. Determination of cell migration by transwell or agarose drop assay. Results: We modulated by transfection the intracellular concentrations of cofilin and Tβ4 of two colon (3LNLN and EB3) and one breast carcinoma (MDA-MB-231) cell line and analyzed their migratory activity. Increasing wild-type cofilin did not alter their migratory activity, whereas the constitutively active S3A-cofilin mutant elevated migration. Transfection leading to an up- or downregulation of Tβ4 showed that MDA-MB-231 and 3LNLN cells responded with a decrease or increase in migration, respectively. Exposure of MDA-MB-231 and 3LNLN cells to increasing concentrations of extracellular Tβ4 (or His-tagged Tβ4) induced a biphasic response of migration, being highest around 0.24 μM and decreased at higher extracellular Tβ4. Immunostaining of 3LNLN cells exposed to 0.24 μM extracellular His-tagged Tβ4 with anti-His antibody indicated its uptake co-localizing with integrin-linked kinase at cell attachment points. Furthermore, the exposure to 0.24 μM His-tagged Tβ4 led to increased phosphorylation of AKT1/2 and secretion of matrix metalloproteases. These effects and tumor cell migration were abrogated after exposure of 3LNLN cells to 2.8 μM His-Tβ4, also inducing apoptosis in a number of cells. Conclusions: Tumor cell migration can be inhibited by high extracellular Tβ4.

Keywords: actin; carcinoma cells; cofilin; integrin-linked kinase; thymosin beta



Academic Editor: Ewa Grzybowska

Received: 27 December 2024

Revised: 4 April 2025

Accepted: 8 April 2025

Published: 18 April 2025

Citation: Al Haj, A.; Ćwikłowska, K.; Mazur, A.J.; Brand-Saberi, B.; Hannappel, E.; Mannherz, H.G. Concentration-Dependent Pleiotropic Effects of Thymosin Beta4 and Cofilin on the Migratory Activity of Carcinoma Cells. *Int. J. Transl. Med.* **2025**, *5*, 16. <https://doi.org/10.3390/ijtm5020016>

Copyright: © 2025 by the authors. Licensee MDPI, Basel, Switzerland. This article is an open access article distributed under the terms and conditions of the Creative Commons Attribution (CC BY) license (<https://creativecommons.org/licenses/by/4.0/>).

1. Introduction

Tumor malignancy defines the ability of tumor cells to metastasize and to form daughter tumors. Metastasis is the main cause of death in cancer patients. Most solid tumors arise from epithelial tissues. After undergoing extensive reprogramming initiated and supported by a multitude of external signals from the tumor micro-environment, tumor cells arise

after undergoing the so-called epithelial-to-mesenchymal transition (EMT), leading to the re-establishment of the ability for active migration. Metastatic tumor cells migrate out from their original organ or tissue as single cells or clusters, using either the amoeboid or mesenchymal (or fibroblastic) form of locomotion [1,2]. They traverse multiple barriers of the extracellular matrix (ECM), such as compact basement membranes or net-like structures formed by ECM fibrils, in order to invade vessels and finally extravasate into distant organs, where they may form new solid tumors [for reviews, see [1–3]. Independent of the mode of migration, metastasis of tumor cells depends on dynamic alterations of their cytoskeleton, in particular, of the actin filament system.

Actin itself is a protein of 42 kDa molecular mass and cycles between two main states: the monomeric and filamentous forms termed G-actin and F-actin, respectively [4,5]. In quiescent cells, about 50% of the actin is maintained in the monomeric state, stabilized by G-actin-binding proteins like thymosin beta4 (T β 4) or profilin, or transiently by cofilin/ADF [6–10]. During active cell migration, however, the equilibrium between G- and F-actin is shifted towards the filamentous form. Actin filament bundles form the cores of specific protrusions at the cellular fronts to generate protrusive forces: invadopodia (invasive protrusions), filopodia, lamellipodia, and blebs [11–13]. Invadopodia enable tumor cells to also secrete proteolytic enzymes, mostly matrix metalloproteases, which degrade extracellular matrix (ECM) components to facilitate tumor cell migration [14,15]. Filopodia and lamellipodia are plasma membrane extensions formed in the direction of the movement by cells exhibiting the fibroblastic type of migration, whereas blebs are typical for amoeboid cells migrating through dense ECM networks [16].

The directional movement of metastatic cells is determined by specific plasma membrane extensions, the filopodia and lamellipodia. Their propulsive movement is achieved by actin treadmilling that depends on the different properties of the actin filament ends [17,18], whose plus ends are attached to the plasma membrane and elongate by preferential addition of new actin subunits, generating the force necessary for its propulsion [18]. Simultaneously, actin subunits are released from their minus ends that extend towards the cytoplasm [17,18]. Thus, treadmilling generates the force necessary for the forward translocation of the plasma membrane. In addition, these plasma membrane extensions explore the surroundings of the migrating cell and attach to particular ECM components via integrin receptors [18]. Finally, the more stable F-actin networks at the posterior parts of the migrating cell interact with short myosin filaments to generate the forces necessary for the retraction of the trailing cell body [16,18].

In contrast, when cells move through a dense three-dimensional network of extracellular components, they switch to the amoeboid type of movement, which is independent of adhesions to ECM components and characterized by rapid shape changes in the migrating cell and the formation of bleb-like extensions, caused by localized disassembly of the sub-membranous cortical F-actin and cytoplasmic pressure generated by force-producing actin–myosin interactions [2,16]. The blebs seem to search for spaces within the ECM network allowing a squeezing passage powered by actin–myosin interactions. Many metastatic tumor cells can rapidly switch between these modes of migration [2,16]. Though both modes of metastatic cell migration (amoeboid or fibroblastic) may be differently regulated, they both depend on the basic dynamic behavior of the actin filament system, whose dis- and re-assembly and treadmilling within the protrusions is regulated by a large number of actin-binding proteins (ABPs) [4,5,19].

The members of the ADF/cofilin protein family stimulate actin cycling by their ability to fragment F-actin (at a low relative concentration to F-actin) or promote actin subunit dissociation from the slow-growing minus ends of F-actin, leading to stimulation of cell migration [20,21]. A number of reports have also shown that the ubiquitous non-muscle

cofilin-1 variant is overexpressed in metastatic tumor cells, and by severing F-actin, it may lead to numerous short actin filaments exposing free plus-ends that induce the formation of new actin filaments [22,23].

The beta-thymosins are small peptides of 43 amino acid residues. In aqueous solutions, T β 4 behaves like an intrinsically unstructured protein, but when bound to G-actin, it attains a conformation characterized by N- and C-terminal α -helices connected by a flexible loop, allowing it to span from the bottom of the actin subdomain-1 to the top of subdomain-2 [24,25]. This particular mode of T β 4 binding to actin results in inhibition of actin polymerization. Intracellularly, the high K_D of this complex (about 1 μ M) establishes an equilibrium among F-actin, T β 4-complexed actin, and a “pool” of non-T β 4-complexed and reusable G-actin. Consequently, actin polymerization leads to a reduction of the pool of reusable actin that is compensated by the dissociation of actin complexed to T β 4. Indeed, activated nucleating proteins (like the formins or Arp2/3 complex) that promote actin polymerization [26,27] will consume and reduce the concentration of “reusable” G-actin and thereby indirectly induce the dissociation of the actin:T β 4 complex in order to maintain the equilibrium between free and T β 4-bound G-actin. Conversely, an increase in the intracellular concentration of T β 4 will lead to a rise of the fraction of T β 4-sequestered actin. A possible reduction of the reusable actin pool will be compensated by disassembly of existing actin filaments. Indeed, it has been demonstrated that HeLa cells overexpressing T β 4 have a reduced number of microfilaments and therefore a reduced rate of migration, whereas cells with lowered T β 4 content showed a higher rate of cell migration [28].

In contrast, conflicting results have been reported about the effect of T β 4 on the migratory activity of carcinoma cells. Thus, it was often not possible to define a consistent correlation of their migratory activity with the expression of T β 4, even in tumor cell lines derived from the same organ, like the colon [29–31]. These contradictory results may be due to different ratios of T β 4 to actin or varying concentrations of additional actin-binding proteins like cofilin/ADE, since T β 4 cooperates with these proteins during F-actin disassembly [28]. Therefore, we investigated whether the modulation of the intracellular concentration of cofilin-1 (subsequently termed only cofilin) and, in particular, of T β 4 affected the migratory activity of tumor cells with different metastatic potential, i.e., of cells possessing a different intrinsic potential for active migration. To this end, we selected three established tumor cell lines: the MDA-MB-231 cells derived from triple-negative breast carcinoma and the 3LNLN and EB3 lines derived from colon carcinoma [32] possessing high, intermediate, and low migratory activity, respectively. These cell lines were analyzed by investigating the dependence of their migratory activity before and after modulation of their intracellular cofilin concentration by transfection with wild-type or mutant variants of cofilin. Our data show that overexpression of wild-type cofilin had only a small effect on the migration of the MDA-MB-231, 3LNLN, and EB3 cells. Only transfecting the constitutively active S3A-cofilin mutant stimulated migration of the MDA-MB-231 cells.

In contrast to cofilin, up- or downregulation of the intracellular T β 4 concentration by transfection led to the reduction or stimulation of tumor cell migration, respectively. In addition, we analyzed the effect of extracellular native or His-tagged T β 4 on the migration of the selected tumor cells. Surprisingly, these data showed a biphasic response of their migratory activity when exposed to increasing T β 4: a stimulation of migration by up to 0.24 μ M extracellular T β 4 and an inhibition at higher (2.4 μ M) T β 4 concentrations. Anti-His and -T β 4 immunostaining indicated that extracellular His-T β 4 was taken up by the exposed colon tumor cells, leading at 2.4 μ M to cell rounding caused by F-actin microfilament disassembly and subsequent apoptosis.

These data showed that the migratory activity of the selected cells was clearly modified by alterations of the T β 4 concentration, though high-performance liquid chromatography

(HPLC) analysis showed that they also contained the beta-thymosin variant T β 10. T β 10 was previously shown to be especially expressed in tumor cells with highly malignant neoplastic phenotypes [33,34]. Recent data, however, have shown that T β 4 and T β 10 possess identical actin-sequestering activity and modify in synergy the intracellular equilibrium of monomeric-to-filamentous actin [35,36]. Since our immunodot data indicated that the used anti-T β 4 antibody also recognizes T β 10, albeit weaker than T β 4, we are confident that our results are not modified by a beta-thymosin variant with different properties but occurred at an endogenous background of actin-sequestering activities effected by both T β 4 and T β 10.

Further experiments were performed to analyze the possible signaling pathways initiated by migration stimulating or inhibiting T β 4 concentrations. Thus, we demonstrate by immunostaining co-localization of T β 4 with the integrin-linked kinase (ILK). Previous data had shown that T β 4 binding to the LIM-domain-containing PINCH protein induced the formation of a supramolecular complex, with ILK and parvin leading to ILK activation and subsequent phosphorylation and activation of the AKT/PKB (protein kinase B) signaling pathway [37,38]. Indeed, immunostaining 3LNLN colon carcinoma cells exposed to 0.24 μ M T β 4 for phosphorylated AKT/PKB indicated an increase in P-Ser473-AKT-1 and P-Ser474-AKT-2 immunoreactivities, which are known to stimulate cell migration and secretion of metalloproteases ((MMPs) [39]). Indeed, at 0.24 μ M extracellular T β 4, we detected increased MMP expression and secretion. In contrast, exposure of 3LNLN cells to 2.8 μ M His-tagged T β 4 led to cell rounding, inhibition of migration, and induction of apoptosis of many cells.

2. Materials and Methods

2.1. Materials

Fetal calf serum (FCS) and media were obtained from Gibco (Thermo Fisher Scientific, Schwerte, Germany). The monoclonal anti- β -actin antibody (clone AC74) was purchased from Sigma (Poole, Dorset, UK) and FITC-labeled anti-rabbit IgG from Amersham Biosciences (Freiburg, Germany). TRITC-phalloidin was obtained from Molecular Probes (Eugene, OR, USA). The specificity of the polyclonal antibody against cofilin generated in rabbits was described previously [40]. The monoclonal anti-T β 4 antibody was a commercial product by the BS-Antibody Facility of TU Braunschweig (Braunschweig, Germany) and kindly provided by Prof. Brigitte Jockusch and Mrs. R. Buchmeier (TU Braunschweig, Germany). Its properties have been described previously [28]. In addition, we tested the specificity of this anti-T β 4 antibody by immunodot blots. An analysis of its reactivity against T β 4, bovine T β 9, and T β 10 indicated a stronger reactivity towards T β 4 than to T β 9 and T β 10 (see Supplementary Materials Figure S1), probably due to the fact that T β 9 and T β 10 differ from T β 4 by 8 and 11 exchanges, respectively [35,36]. Antibodies against integrin-linked kinase (ILK) were from Merck-Millipore (Darmstadt, Germany); antibodies against AKT-1,2 (goat) and phospho-S473-AKT-2 (rabbit) were from Santa Cruz Biotechnology (Heidelberg, Germany); and the antibody against phospho-S474-AKT2 was from SAB Biotherapeutics (Washington, DC, USA). The anti-MMP2 (EPR1184), -MMP9 (RM120), and -TIMP2 Anti-TIMP2 (F27P3A4) antibodies were from Abcam Limited, Cambridge, UK. The anti-His antibody (rabbit) was from MicroMol (Karlsruhe, Germany).

The vectors leading to independent overexpression of T β 4 and EGFP (pIRES2-EGFP-Express) and to T β 4 downregulation by T β 4-specific shRNA were described previously [41,42]. Pre-stained molecular mass standard (PageRuler) was obtained from Fermentas (St. Leon-Rot, Germany). Matrigel was obtained from BD Biosciences (Heidelberg, Germany). All other reagents were of analytical grade.

2.2. Cell Lines, Cell Culture, and Transfection Vectors

Colon adenocarcinoma and the breast cancer MDA-MB-231 cell lines of human origin were included in this study. The derivation of the EB3 and 3LNLN cells is described elsewhere [32,43]. The Caco-2, SW480, LS174t, HT-29, and MDA-MB-231 cells were from ATCC[®] (Teddington, UK). The origin of the tumor cells was determined by STR profiling. The culture of tumor cell lines was performed as described previously [43]. Cells grown on sterile glass coverslips in DMEM with added NCS and FCS were fixed with 4% formaldehyde for 20 min, permeabilized with 0.2% Triton X-100 in PBS for 5–10 min, or alternatively fixed with ice cold methanol for 5 min, and subsequently washed three times in PBS.

Cell transfection was performed using vector-coated magnetic beads (MATra, IBA, Göttingen, Germany) using the wild-type and S3A- and S3D-cofilin constructs cloned into the BglII-EcoRI site of the vector pEGFP-C2 (obtained from BD Clontech UK, Basingstoke, UK), as described previously [28]. The bicistronic T β 4-pIRES2-EGFP and T β 4-shRNA-EGFP constructs were obtained as stated in [41,42]. For T β 4 knockdown, we used T β 4-specific (short-hairpin) shRNAs, which were selected to target the following sequences of the human T β 4 mRNA (accession code TMSB4X), starting from position 103 (GAGATCGAGAAATTCGATA), 195 (GCAAGCAGGCGAATCGTAA), 472 (GACGACAGTCAAATCTAGA), or 526 (GTAATGCAGTTTAATCAGA). Oligonucleotides coding for shRNA molecules were produced by Invitrogen (Karlsruhe, Germany) and cloned under control of the H1 or U6 promoter into an EGFP co-expressing vector generated by [42]. To enhance knockdown efficiency, we used in some experiments a mixture of all four vectors for transfection.

2.3. Cell Migration Assays and Immunofluorescence Microscopy

Transwell cell migration of transfected and non-transfected tumor cells was performed by using Transwell[™] filters (BD Biosciences, Heidelberg, Germany), as described previously [28]. Briefly, cells starved for six hours were taken up in serum-free medium supplemented with 0.2 mg/mL Matrigel, seeded into a Boyden chamber, and subsequently placed into a well, whose bottom had been coated with a mixture composed of 50% (=5 mg/mL) Matrigel, 20% FCS, and 30% medium.

As an alternative procedure to follow cell migration, we used the agarose drop assay [44]. For this assay, 50,000 cells were mixed with 4 μ L of 2% agarose and placed in the middle of a well of a 96-well plate after determination of the percentage of transfection. After 72 h, the cells migrating out of the agarose drop were photographed using a confocal microscope. For immunohistochemistry of the migrating cells, the agarose drops were placed on glass coverslips coated with 0.5 mg/mL laminin. For immunostaining, the cells were fixed for 10 min with 4% paraformaldehyde and subsequently immunostained, as detailed previously [28]. Immunofluorescence microscopy was performed by using either a Zeiss Axiophot microscope equipped with an AxioCam HRc digital camera or the confocal Zeiss LSM 510 or 800 microscope (Jena, Germany).

2.4. Protein Preparations and Immunoblotting

Thymosin beta 4 was a commercial product from Bachem (Bubendorf, Switzerland), and T β 4, T β 9, and T β 10 were prepared as described [45]. His-tagged T β 4 and His-tagged scrambled T β 4 (scT β 4) were obtained recombinantly, as described [46], and purified using a NiNTA-column (Sigma, Munich, Germany). Protein concentrations were determined by the colorimetric assay, as described [47]. Western and dot blots for the detection of T β 4, ILK, AKT1/2, and phosphorylated AKT were performed as described [40]. Actin as housekeeping protein was detected after stripping the blots with 0.1 M glycine-HCl, pH 3.0, for 30 min at room temperature. Equal loading was tested by immunostaining for β -actin or tubulin. For detection of T β 4, we preferably used dot immunoblots, because comparative

data using Western and immunodot analyses indicated that a considerable amount of T β 4 was lost during electro-transfer from SDS-gels to nitrocellulose membranes for Western blotting (wet transfer using a Protean devise (Biorad, Munich, Germany)). The results indicated differences between Western and dot immunoblots, even though applying equal protein amounts (50 μ g/lane or dot), possibly due to transmigration of T β 4 through the membrane during the electro-transfer.

2.5. Determination of the Intracellular Beta-Thymosin Content by Reverse-Phase High-Performance Liquid Chromatography (HPLC) After Equilibrium Centrifugation

We determined the intracellular beta-thymosin concentration in a number of tumor cells, in particular, in MDA-MB-231, 3LNLN, and EB3 cells, by HPLC separation (reverse-phase high-performance liquid chromatography) [48]. For this determination, the intracellular proteins were prepared from 10^7 to 7×10^7 cells according to the published procedure and analyzed by HPLC. The concentrations of beta-thymosins and fragments were determined as described [48]. Briefly, the top 50 μ L from centrifugation assays were mixed with 5 μ L 4 M perchloric acid and incubated for 30 min at 4 °C. After centrifugation at $20,000 \times g$ for 5 min, the supernatant solution was carefully removed. The supernatant solution was adjusted to pH 3–5 with 10 M KOH. After 15 min on ice, the precipitated KClO₄ was removed by centrifugation, and an aliquot of the supernatant solution was analyzed by HPLC. Chromatographic conditions were flow rate of 0.75 mL/min and buffer of 0.11 M pyridine plus 0.076 M acetic acid. The peptides were eluted by a linear gradient from 0 to 40% n-propanol in 30 min using a Beckman ODS Ultrasphere column (4.6 mm \times 250 mm); post-column derivatization was with fluorecamine. Chromatographic conditions were controlled by a Beckman 420 fluorometer with 365 nm excitation from an FSA 110 lamp with no excitation filter and an FS 426 emission filter with a cut-off below 418 nm [48]. The fluorescence signal was registered on an integrator (Merck-Hitachi). For the ODS Ultrasphere column, the retention volumes of T β 4 and T β 10 and the determination of their concentrations were calibrated by applying defined concentrations of purified T β 4 and T β 10. Supplementary Materials Figure S2A provides a HPLC elution profile after applying 200 ng of T β 4 and T β 10 to demonstrate clear separation of both beta-thymosins. Subsequently, the concentration of the eluted beta-thymosins present in cell homogenates was calculated from their peak areas [49].

3. Results

3.1. The Distribution of T β 4 and Organization of the Actin Cytoskeleton in Tumor Cell Lines

We have previously shown for HeLa cells that T β 4 co-localizes with actin filaments at the sites of their attachment to the cell membrane [28]. Here, we analyzed by immunohistochemistry the distribution of T β 4 and the organization of the actin cytoskeleton in a number of human colon carcinoma cell lines (HT-29, LS174t, Caco-2, SW480, EB3, and 3LNLN) and the breast carcinoma cell line MDA-MB-231. Figure 1 shows the distribution of T β 4 in relation to the microfilaments of the MDA-MB-231 and the colon tumor EB3 and 3LNLN cell lines. TRITC-phalloidin staining demonstrated short peripheral stress fibers in MDA-MB-231 and 3LNLN cells, which peripherally converged, suggesting the presence of focal adhesions (Figure 1A, arrows). The 3LNLN cells contained numerous but more punctate TRITC-phalloidin-positive structures (Figure 1B), like the sessile EB3 cells (Figure 1C), which showed a strong, dotted anti-T β 4 staining overlaying a more dot-like TRITC-phalloidin distribution (arrows in Figure 1C). Anti-T β 4 staining revealed a more perinuclear concentration in MDA-MB-231 cells (Figure 1A), but an almost even cytoplasmic staining in 3LNLN and EB3 cells (Figure 1B,C). F-actin-containing structures were observed in MDA-MB-231 and 3LNLN cells (Figure 1A,B) but appeared absent in

EB3 cells (Figure 1C). The anti-T β 4 staining showed T β 4-positive dots along presumed stress fibers in MDA-MB-231 (arrow in Figure 1A) that were more prominent in 3LNLN cells (Figure 1B). Anti-T β 4-stained dots were detected in EB3 cells, completely filling their cytoplasm, which in some instances coalesced to larger aggregates (arrow in Figure 1C). The T β 4-positive dots appeared to co-localize in many instances with TRITC-phalloidin-positive dots (Figure 1B,C), suggesting the presence of only short or oligomeric actin filaments. In most cases, the cell nuclei were free of anti-T β 4 staining.

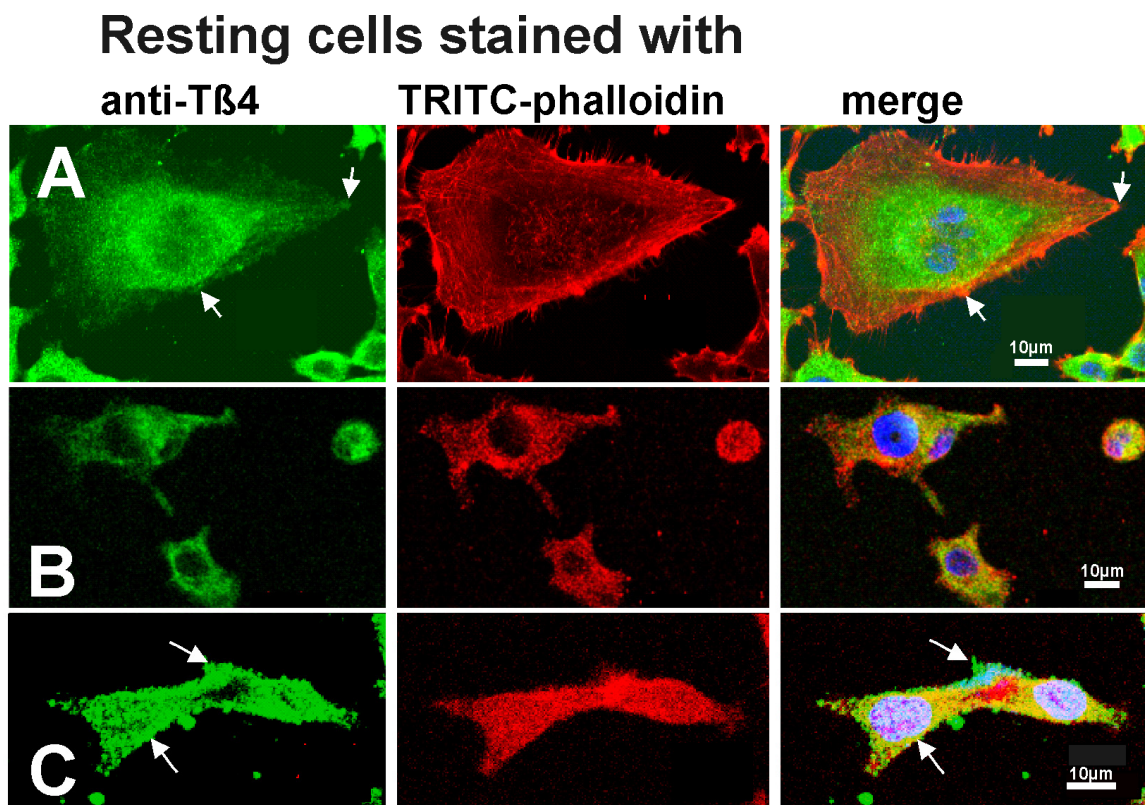


Figure 1. Immunostaining with anti-T β 4 and TRITC-phalloidin of (A) MDA-MB-231. Arrows point to focal adhesions formed by converging microfilaments and an accumulation of anti-T β 4 staining, (B) 3LNLN, and (C) EB3 cells. These cells showed a strong punctate accumulation of anti-T β 4 overlaying TRITC-phalloidin stained F-actin areas. Bars represent 10 μ m.

In addition, we analyzed the distribution of F-actin and T β 4 within a number of other colon carcinoma cell lines (Caco-2, SW480, LS174t, and HT-29 cell lines). The data compiled in Supplementary Materials Figure S3 demonstrate a high perinuclear concentration of T β 4 in Caco-2 and SW-480 cells and its even cytoplasmic distribution in LS-174t and HT-29 cells, whereas TRITC-phalloidin-stained F-actin concentrated in the cell periphery of these lines. Microfilaments reaching towards the cell center were only detected in the Caco-2 cells (Figure S3). These cell lines (Caco-2, SW480, LS174t, and HT-29) showed little migratory behavior, probably due to their apparently high concentration of T β 4 (see later and Supplementary Materials Table S1). Therefore, we selected the 3LNLN, EB3, and MDA-MB-231 cell lines to analyze the effects of the modulation of T β 4 and cofilin concentration on their migratory activity.

3.2. Effect of Cofilin Overexpression on Tumor Cell Migration

Cell migration depends on constant actin treadmilling, i.e., F-actin disassembly and reassembly. F-actin treadmilling is stimulated by proteins of the ADF/cofilin family, which are F-actin-severing and cycling-accelerating proteins and secure a constant supply of

polymerization-competent monomeric actin [20,21]. Since previous data had indicated for HeLa cells that cofilin and T β 4 cooperate synergistically in the depolymerization of F-actin [28], we first investigated whether the different migration behavior of the three selected tumor cells was due to different levels of cofilin expression. Immunodot blots of homogenates of the three cell lines, however, showed an almost identical content of cofilin-1 in MDA-MB-231, 3LNLN, and EB3 cells (see Supplementary Materials Figure S4A). Setting the content in MDA-MB-231 cells to 100%, then cofilin expression amounted to 113% in 3LNLN and 98% in EB3 cells. These data suggested that the differing migratory activity of these cells was not due to differences in cofilin expression.

Nevertheless, we analyzed whether modulation of the active state of the intracellular cofilin concentration modified the migratory activity of these tumor cells. Cofilin activity is intracellularly regulated by phosphorylation of Ser3 by ROCK-dependent LIM kinase, resulting in inhibition of its actin-binding capacity [50]. Dephosphorylation by, for instance, the slingshot phosphatase reactivates its actin-binding activity [50]. Three constructs N-terminally fused to EGFP [41] were employed: human wt-cofilin and the constitutively active S4A and inactive S3D variant. Successful transfection was indicated by EGFP-fluorescence and was about 15% of the total cells employed. The alterations in cofilin expression were analyzed 24 h after transfection for the 3LNLN cells by immunoblots using the polyclonal anti-cofilin antibody, which does not discriminate between the different mutant forms. In 3LNLN cells, we obtained increases in total cofilin expression of 156% and 198% after transfection with wt- and the S3A variant, respectively, over the endogenous cofilin, i.e., after transfection with the empty EGFP vector (see Supplementary Materials Figure S4E). After determination of the percentage of EGFP-positive cells 24 h after transfection, they were loaded on a transwell chamber, and the number of migrating cells was quantified after a further 24 h calculating the migration ratios for the transfected, EGFP-positive cells. The EB3 line did not respond to an overexpression of these cofilin constructs (Figure S4D). Overexpression of wt-cofilin had no effect on the migration of both the MDA-MB-231 and 3LNLN cells, which might be explained by the assumption that the intracellular kinases (such as LIM-kinase; see [50]) rapidly phosphorylated the overexpressed wt-cofilin and thereby re-established the initial equilibrium between the de- and phosphorylated cofilin. In contrast, transfection with the active S3A-cofilin construct clearly stimulated the migratory activity of MDA-MB-231 but had only a small stimulatory effect on 3LNLN and no effect on EB3 cells (Figure S4B–D). Since the constitutively active S3A-cofilin mutant cannot be phosphorylated, its overexpression might have led to increased F-actin-severing activity, resulting in an increase in filament ends, which are known to promote cell migration by increasing actin cycling [9,10]. This effect, however, was only observed for the MDA-MB-231 cells. In contrast, the 3LNLN and EB3 cell lines may have contained lower amounts of F-actin ready for fragmentation by S3A-cofilin, as neither wt- nor S3A-cofilin transfection of 3LNLN and EB3 cells led to a significant alteration of their migratory behavior. Furthermore, our data showed that the constitutively inactive S3D-cofilin had no effect on the migratory activity of all three cell lines. Thus, these data indicated that an intracellular increase in the constitutively active S3A-cofilin increased the migratory activity of only the MDA-MB-231 cells, whereas transfection of wt-cofilin had no effect.

Of note, compared to non-transfected 3LNLN cells (set at 100%), transfection with wt-cofilin and S3A-cofilin led to an increase of 123% and 134%, respectively, in their intracellular content of T β 4 (see Figure S4F), suggesting that the possible increase in the migratory activity was counter-regulated by an increase in the T β 4 concentration (see below).

3.3. Effect of Modulating the Intracellular Tβ4 Concentration on Tumor Cell Migration Analyzed by the Transwell Assay

In order to determine the intracellular concentrations of Tβ4 in MDA-MB-231, 3LNLN, and EB3 cells, we initially compared Western and immunodot blotting (Figure 2A). As detailed in the Section 2, our data indicated more reliable results using the immunodot procedure. Densitometric evaluation of the immunodot data (Figure 2A) showed that the endogenous Tβ4 content in MDA-MB-231 cells was lowest, i.e., in the cells with the highest migratory activity. When the Tβ4 content in MDA-MB-231 cells was set at 100%, then the Tβ4 expression increased to 133% and 156% in 3LNLN and EB3 cells, respectively, over the content in MDA-MB-231 cells (Figure 2A). These data showed considerable differences in the Tβ4 expression by these tumor cells and suggested an inverse correlation of Tβ4 expression and their migratory activity.

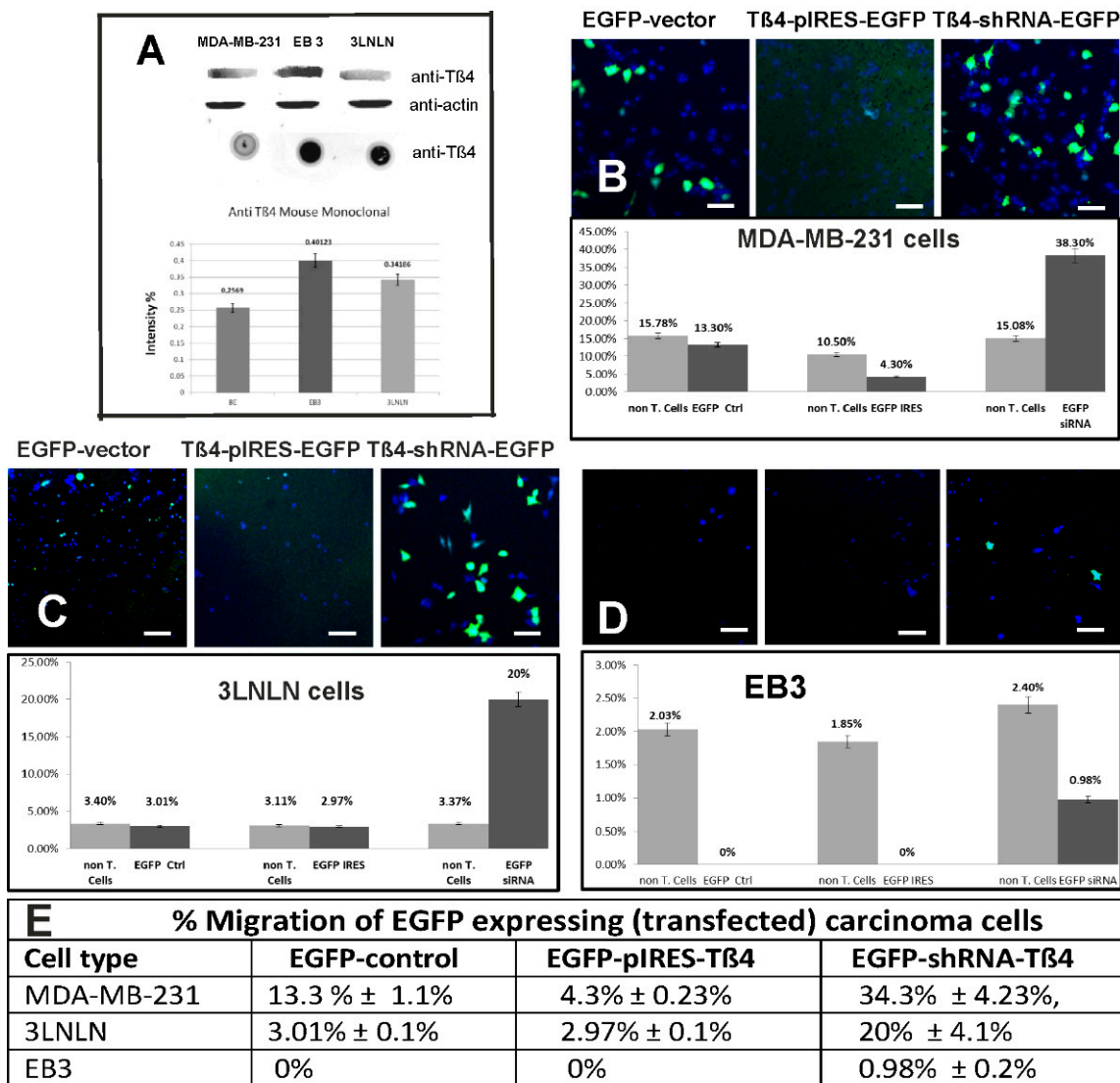


Figure 2. Effect of the modulation of the Tβ4 concentration by transfection on tumor cell migration. (A) Anti-Tβ4 Western and immunodot blots of homogenates of the MDA-MB-231, EB3, and 3LNLN cells using mouse monoclonal anti-Tβ4 (immunodot analysis was repeated five times). To demonstrate the monospecificity of the anti-Tβ4 antibody, a complete Western blot is shown in Supplementary Materials Figure S5A, displaying an apparent Mr of 5 kDa. After stripping the blot (see Section 2),

the application of identical amounts of homogenates was verified by an anti-actin Western blot. Note the differences in immunoreactivity between Western and immunodot blots (for further details, see text). Using an arbitrary scale the immunodot intensities were determined to be 0.255, 0.41, and 0.342 for MDA-MB-231, EB3, and 3LNLN cells respectively. Setting the highest value (EB3 cells) to 100%, this results to a relative T β 4 concentration in MDA-MB-231 and 3LNLN cells of 63.5% and 85%, respectively, in good agreement with the HPLC data (see Table 1, total β -thymosins). (B–D) Quantitation of cell migration of the three tumor cell lines by using the transwell assay (Boyden chamber). Cells were transfected with vectors leading to expression of only EGFP, with pIRES-T β 4 leading to overexpression of T β 4 and with T β 4-specific-siRNA as described in Materials and Methods. Twenty-four hours after transfection, 50,000 cells were loaded on the transwell insert and further treated as described. After a further 24 h, the number of cells migrated through the transwell membrane was counted. Transfected cells were identified by EGFP-fluorescence (dark-grey columns) and non-transfected cells (light-grey columns) by Hoechst 33342 nuclear stain using confocal microscopy (for detailed numbers see text). Images depict representative areas showing migrated cells: (B) MDA-MB-231 cells; (C) 3LNLN cells; and (D) EB3 cells. The percental evaluation (% migrated cells of total number of cells applied: 50,000) together with the standard deviations from four independent experiments of the different conditions is shown in the graphs below the confocal images. Note the different scaling of the ordinates showing percental migration. Note that transfection with a vector leading to expression of only EGFP led to only a slight reduction of the migration of the control, i.e., of non-transfected cells (denoted as non-T. cells). (E) Table compiling the percental migration activity (\pm standard deviations, as shown in the figures, from four different experiments) of transfected, i.e., EGFP-expressing, cells. (B–D) Bars correspond to 50 μ m.

Table 1. Calculation of the intracellular beta-thymosin concentrations in the three cell lines as determined by HPLC (mean values from two measurements). For original HPLC data, see Supplementary Materials Figure S2.

EB3	3LNLN	MDA-MB-231	Cell Type
0.466 μ M	0.33 μ M	0.306 μ M	Intracellular T β 4
0.66 μ M	0.62 μ M	0.353 μ M	Intracellular T β 10
1.126 μ M	0.95 μ M	0.659 μ M	Total β -thymosins

Finally, we determined by HPLC the beta-thymosin content of MDA-MB-231, EB3, and 3LNLN cells (see Section 2 and Supplementary Materials Figure S2). The data summarized in Table 1 indicate that both cell lines contain two variants of beta-thymosin: T β 4 and T β 10. T β 10 possesses G-actin-sequestering activity identical to T β 4 [33,34], but divergent properties have been attributed to both variants. T β 10 is upregulated in many cancer cell types and regarded as a sign for poor prognosis [35,36]. T β 4 and T β 10 differ by 11 amino residue exchanges [51] and are coded by different genes located on the X-chromosome and chromosome 2, respectively [33]. Therefore, it is highly likely that they are differently regulated and the T β 4-specific clones employed only target T β 4-mRNA.

Applying defined numbers of cells for the HPLC analysis (Supplementary Materials Figure S2), the obtained data allowed determining the amount of beta-thymosins in femtomole/cell. Under the assumption that the cell volume of these cells was 3000 μ m³, as shown for many tumor cells like HeLa cells [51], the intracellular concentrations of T β 4 and T β 10 were calculated as shown in (Table 1), although we are aware that the volumes of the three cells selected may vary and furthermore change according to their activities, as reported for HeLa cells [49], and no correction was made for the nuclear volume. Setting again the content of beta-thymosins in EB3 cells to 100%, then the relative total content of beta-thymosins in MDA-MB-231 cells was 58.5% and in 3LNLN cells 84.4%; in good agreement with the immunodot data (see legend to Figure 2A). Furthermore, this result

indicates that the monoclonal anti-T β 4 antibody does not differentiate between T β 4 and T β 10 (see immunodot in Supplementary Materials Figure S1).

Next, we analyzed the effect of the intracellular T β 4 concentration on the migratory behavior of these three tumor cell lines by modulating its intracellular concentration by transfection with constructs, which led to overexpression or downregulation of T β 4. To this end, we employed a bicistronic T β 4-pIRES-EGFP construct [41], leading to an independent overexpression of T β 4 and EGFP, and a T β 4-specific shRNA construct that downregulates T β 4 but induces EGFP expression (T β 4-shRNA-EGFP) [42], allowing in both cases the identification of successful transfection. Transfection with the T β 4-pIRES-EGFP construct should have led to an increase in T β 4 expression in the EGFP-positive cells, whereas transfection with T β 4-shRNA-EGFP might have resulted in an intracellular reduction of only T β 4.

We observed clear inhibitory and stimulating effects, respectively, on their migratory activity (as summarized in Figure 2E). After transfection, cell migration was tested by two assays: the transwell procedure using a Boyden chamber and the agarose drop assay (see Materials and Methods). The migratory activity of the tumor cells was determined 24 h after transfection by calculating the ratios of the number of migrated/applied non-transfected or transfected cells based on the presence or absence of EGFP-fluorescence.

First, we tested the migratory activity of the three selected cell lines using the transwell (Boyden chamber), which also allowed a quantification of the data. The data showed that the MDA-MB-231 cells had the highest; the 3LNLN cells an intermediate; and the EB3 cells the lowest, i.e., practically none, migratory activity (Figure 2B–D), correlating inversely with their intracellular content of T β 4. We also compared for each condition the cell migration for non-transfected and transfected cells. The transwell assay showed in four independent experiments migration through the transwell membrane of $13.78\% \pm 1.1\%$ for non-transfected and $13.3\% \pm 1.1\%$ for EGFP-control transfected MDA-MB-231 cells; $3.29\% \pm 0.37\%$ of the non-transfected and $3.01\% \pm 0.1\%$ EGFP-control transfected 3LNLN cells; and $2.1\% \pm 0.25\%$ of the non-transfected and 0% of the EGFP-control transfected EB3 cells (Figure 2B–D), suggesting only a small inhibitory effect of the transfection procedure. Next, we determined the effect of modulating the intracellular T β 4 concentration by transfection. The migration ratios were determined for the transfected EGFP-positive cells. Four independent experiments were performed for each condition, with about 10% transfection yield. Figure 2E Table summarizes the percental migration activity (\pm standard deviations) of the three cell lines after transfection with EGFP-control, EGFP-pIRES-T β 4, or EGFP-shRNA-T β 4 vector leading to no additional, increase or reduction of T β 4 expression, respectively. Transfected cells were identified by their EGFP-fluorescence.

The data obtained indicated that overexpression of T β 4 reduced and its downregulation increased the migratory activity of these tumor cells when compared to cells transfected with the empty T β 4-pIRES-EGFP vector as the control (Figure 2B–D). Furthermore, the data obtained showed that the tumor cells responded to different extents to the modulation of the intracellular T β 4 concentration. Cell lines with high initial migratory activity were more strongly affected by the decrease or increase in intracellular T β 4 concentration. Overexpression of T β 4 reduced the migratory activity of MDA-MB-231 cells to $4.3\% \pm 0.23\%$ of the total EGFP-positive transfected cells, i.e., to 32% of the control, whereas downregulation increased their migratory activity to $38.3\% \pm 4.23\%$, i.e., to 288% of the control (Figure 2B). T β 4 overexpression in 3LNLN cells had only a small reducing effect (to 98% of control), but downregulation a large stimulating effect on their migratory activity (660% of control; see Figure 2C). Principally, similar behavior was observed for the more sessile EB3 cells: few EB3 cells migrated when not transfected, but no migration was observed after transfection with empty EGFP- or T β 4-pIRES-EGFP vector, whereas after transfection with T β 4-shRNA-

EGFP, about 1% of the transfected cells migrated, though the total number of migrating EB3 cells remained low (Figure 2D). Thus, these results indicated that the tumor cells responded to T β 4 downregulation with an increase and to T β 4 overexpression with a decrease in their migratory activity, albeit to different extents, suggesting that additional intracellular components or control mechanisms are responsible for their actual migratory activity.

We also tested by the transwell assay the migratory activity of the additionally included colon tumor cells (SW-480, Caco-2, LS174t, and HT-29) under control conditions and after transfection with both vectors. The data obtained (see Table S1) showed very little migratory activity of these cell lines under control conditions. After transfection with T β 4-pIRES-EGFP, the Caco-2, LS174t, and HT-29 cells showed a slight reduction of their migratory activity, whereas SW-480 hardly responded (Table S1). Transfection with the T β 4-shRNA-EGFP vector led to an increase in the migratory activity of all these cells, though to very different extents (Table S1). Since we assumed that these cells may contain high amounts of beta-thymosins, leading to reduced migration under control conditions, we concentrated in the further analysis on the MDA-MB-231, 3LNLN, and EB3 cells, which exhibited high, intermediate, and reduced migratory activity, as shown by the transwell assay, respectively (Figure 2), aiming to investigate the role of T β 4 for the migration of tumor cells with supposed divergent metastatic activity.

3.4. Cell Migration Analyzed by the Agarose Drop Assay

We employed also the so-called agarose drop assay [44] to investigate the migratory behavior of the tumor cells. In an initial test, 50,000 cells transfected with the EGFP-clone alone were included in 4 μ L 2% agarose drops and placed in laminin-coated wells of a 98-well plate. After 72 h, the number of cells migrating out of the agarose drop was estimated. The percentage of total (non-transfected and transfected) cells migrating out of the drop (Figure 3A–C, showing about a quarter of the agarose drops) decreased from MDA-MB-231 (4.4% = 2200 cells) to 3LNLN (3.7% = 1850 cells) and EB3 (0.22% = 110 cells), showing similar behavior as obtained by the transwell assay.

Next, we concentrated on the 3LNLN cells and investigated their migratory activity after transfection with EGFP-plasmid alone, T β 4-pIRES-EGFP leading to T β 4 overexpression, and T β 4-shRNA-EGFP leading to downregulation of T β 4. Figure 3D–G shows their migration out of agarose drops, whose borders are marked by a yellow line. It can be seen that T β 4 overexpression (Figure 3F) leads to a reduction and its downregulation to an increase (Figure 3G) in the number of fluorescent cells migrating out of the agarose drop in comparison to control or only EGFP-transfected cells (Figure 3D,E).

We also counterstained the 3LNLN cells transfected with T β 4-pIRES-EGFP and T β 4-shRNA-EGFP having left the agarose drop by TRITC-phalloidin (Figure 3H,I). The T β 4-pIRES-EGFP-transfected and EGFP-positive 3LNLN cells showed reduced F-actin content (arrow in Figure 3H' pointing to two EGFP-positive cells). In contrast, the T β 4-shRNA-EGFP-transfected 3LNLN cells showed large lamellipodia-like extensions filled by microfilaments sitting on a strongly TRITC-phalloidin-stained rim, indicating the formation of more filamentous actin (arrows in Figure 3I,I'). It was, however, difficult to reliably estimate the number of fluorescent cells leaving the agarose drops, since they often aggregated or migrated as large groups, making an exact cell count impossible (see in particular Figure 3G).

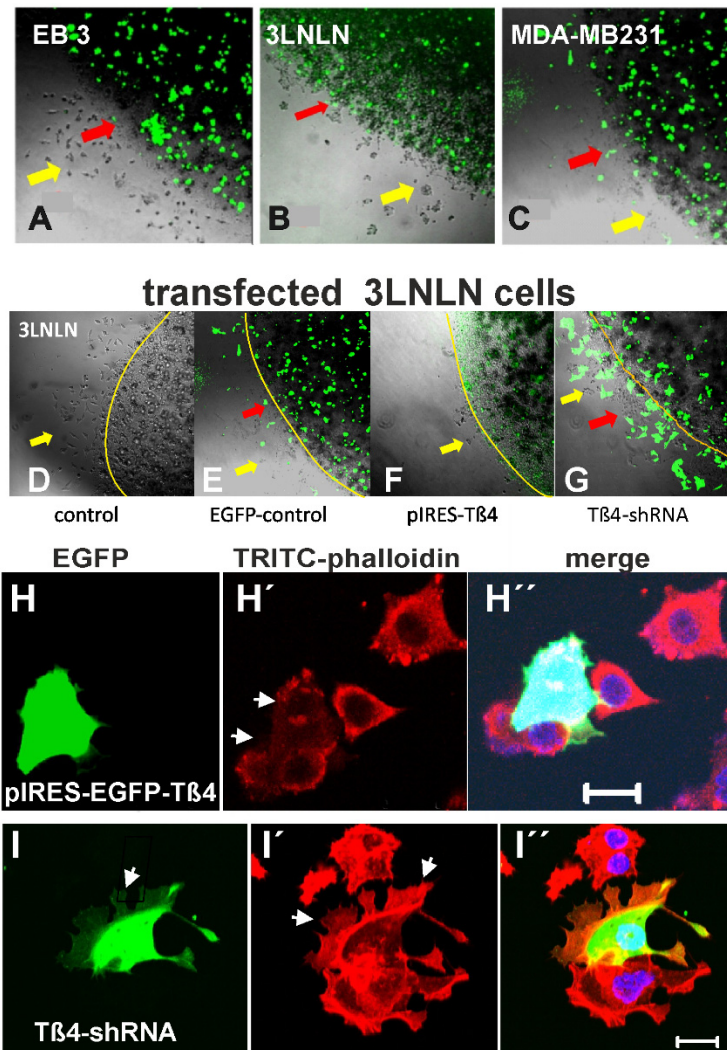


Figure 3. Migration of transfected tumor cells out of agarose drops. Migration of (A) EB3, (B) 3LNLN, and (C) MBA-MB-231 cells after transfection with EGFP-control clone out of agarose drops. For further details, see text. Red arrows point to the margin of the agarose drops and yellow arrows to the agarose free zone, into which the cells migrated. These cells were counted either as non-transfected or as transfected, identified by their EGFP-fluorescence. (D–G) Fifty thousand 3LNLN cells were included in agarose drops 24 h before and after transfection with the Tβ4 vectors indicated (non-transfected (D), EGFP vector (E), pIRES-EGFP-Tβ4 (F), and Tβ4-shRNA-EGFP (G) vector), and after a further 72 h, the cells migrating out of the agarose were photographed using confocal microscopy and counted. Yellow lines depict the boundaries of the agarose drops. Yellow arrows point to non-transfected and red arrows to transfected cells. (H,I) Staining of transfected 3LNLN cells that migrated out of the agarose with TRITC-phalloidin. (H) 3LNLN cells transfected with pIRES-Tβ4, leading to additional expression of EGFP-Tβ4 (EGFP-fluorescence). Note that only two adjacent cells were transfected, i.e., exhibiting EGFP-fluorescence. (H') TRITC-phalloidin staining; note the disassembly of the F-actin cytoskeleton in the transfected (EGFP-positive) cells (arrows). (H'') Gives merged image plus Hoechst 33342 staining. (I) 3LNLN cells transfected with Tβ4-shRNA-EGFP vector. (I') TRITC-phalloidin staining; note the broader lamellipodial structure containing densely packed actin filaments (arrows). (I'') Merged image plus Hoechst 33342. Bars in (A–G) correspond to 50 μm and in (H–I) correspond to 20 μm.

3.5. Influence of Extracellular Tβ4 on Tumor Cell Migration

Next, we analyzed the effect of externally added Tβ4 to tumor cells enclosed in agarose drops on their outwards migratory activity and the organization of their actin filament system, also because earlier reports had indicated that external Tβ4 stimulated the

survival and migratory activity of cardiomyocytes and endothelial cells [37]. Assuming internalization of external T β 4, these published data seemed to contradict our transfection results showing a decrease in migratory activity after upregulation of the intracellular T β 4. Since transient transfection might not lead to a constant alteration of the intracellular T β 4 concentration during the period of observation, we determined the migratory activity of MDA-MB-231 and 3LNLN cells exposed to increasing concentrations of extracellular N-terminally His-tagged T β 4 by the agarose drop assay. The cells having left the agarose drops were counted after 72 h. Both MDA-MB-231 and 3LNLN cells showed an identical biphasic response of their migratory activity to increasing N-terminally His-tagged T β 4 (shown for the 3LNLN cells in Figure 4A and for MDA-MB-231 cells in Supplementary Materials Figure S6), i.e., a stimulatory effect up to an extracellular T β 4 concentration of 0.24 μ M and, thereafter, a gradual decrease reaching the control value (absence of extracellular T β 4) at about 2.8 μ M. Of note, this biphasic behavior was not observed when applying a scrambled T β 4 version (identical amino acid composition but different sequence; Figure 4B). Identical results were obtained for native T β 4, in line with previous data showing that His-tagged T β 4 inhibited actin polymerization like native T β 4 after increasing the salt concentration [46]. In contrast, the EB3 cells did not display a significant response to alterations of the extracellular His-T β 4 concentrations as shown by the transwell assay (Figure 2D).

As the control, we exposed the cells in an identical manner to His-tagged scrambled T β 4 (His-scT β 4; Figure 4B), which was previously shown not to inhibit actin polymerization [48]. His-scT β 4 did not elicit any modifying effect on the migratory activity of the MDA-MB-231 and 3LNLN cells (Figure 4A).

Thus, the MDA-MB-231 and 3LNLN cells showed a biphasic response of their migratory activity to extracellular T β 4: stimulation up to 0.24 μ M His-T β 4 and a gradually increasing inhibition at higher concentrations. At 2.8 μ M extracellular T β 4, many of the 3LNLN cells showed a round morphology (Figure 4F), and the number of both MDA-MB-231 and 3LNLN cells migrating out of the agarose drop had returned to the initial value.

In addition, we investigated whether the tumor cells internalized extracellular His-tagged T β 4. Anti-T β 4 and -His staining suggested its uptake by 3LNLN cells (Figure 4C'). Double immunostaining with anti-T β 4 (green) and anti-His (red) indicated the presence of His-T β 4 in the cytoplasm: concentrated at presumed rear regions but reduced in supposed lamellipodial extensions (arrowheads and arrows in Figure 4C,C'), resulting in a complete co-localization of anti-His (His-T β 4) and anti-T β 4 immunoreactivity (Figure 4C''). When staining F-actin with TRITC-phalloidin, we observed in 3LNLN cells exposed to 0.24 μ M His-T β 4 and after migration out of the agarose drop that most of these cells possessed a well-developed microfilament system terminating in a few cells in weakly T β 4-positive membrane areas resembling lamellipodia (arrowhead in Figure 4D). Figure 4E gives a merge image of a single showing membrane associated accumulation of anti-T β 4 most likely representing adhesion points (arrow in Figure 4E). In addition, we frequently observed cytoplasmic dot-like structures—possibly invadopodia—that were double-positive for T β 4 and F-actin (arrow in Figure 4D'').

Staining the 3LNLN cells exposed to 2.8 μ M His-T β 4 with anti-His for His-T β 4 and TRITC-phalloidin (Figure 4F) showed that most of these cells had attained a round morphology and that His-T β 4 was present within the cytoplasm and weakly within the nuclei, whereas F-actin concentrated in the cell periphery. Thus, these data suggested that cell exposure to 2.8 μ M His-T β 4 had a similar effect as transfection with the pIRES-T β 4 vector, except that all cells were affected.

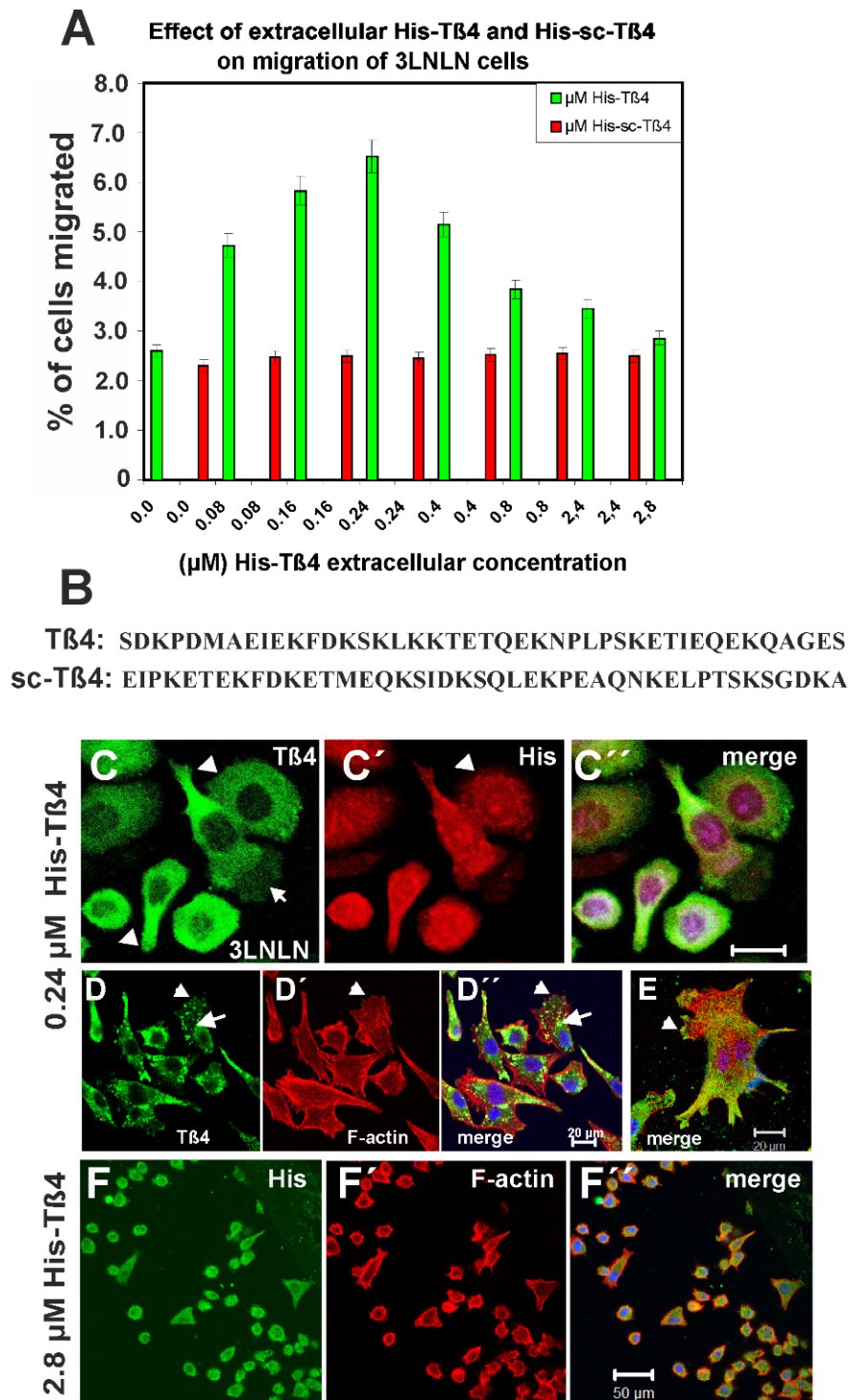


Figure 4. Effect of extracellularly added His-T β 4 or His-scT β 4 (scrambled peptide, negative control) on the migration of 3LNLN cells out of the agarose drops. (A) Depicts the percentages of cells migrated in dependence on the extracellular concentration of His-T β 4 (green bars) and His-scT β 4 (red bars). Note the clear biphasic response to His-T β 4, whereas His-scT β 4 did not elicit any effect. (B) Depicts the sequences of native T β 4 and the scrambled version of T β 4. (C–E) Immunostaining of 3LNLN cells having migrated out of agarose drops at 0.24 μ M His-T β 4 and (F) at 2.8 μ M His-T β 4. (C) Immunostaining with anti-T β 4 (green) and (C') with anti-His (red). (C) Note the high T β 4 concentration within the cytoplasm and the tailing rear (arrowheads), but less intense anti-T β 4 immunoreactivity within a lamellipodium (arrow). (C') Anti-His staining indicated a more perinuclear (arrowhead) and a clear nuclear presence of His-T β 4. (C'') merged image plus Hoechst 33342 staining clearly showing the less intense anti-T β 4 immunoreactivity within a lamellipodium

(arrow in C). (D) Anti-T β 4 staining shows punctate accumulation of anti-T β 4 staining (arrow) that partially co-localizes with (D') TRITC-phalloidin staining also showing a prominent F-actin cytoskeleton concentrating around the cell periphery. (D–D'') Arrowhead points to a presumed lamellipodium. (D'') Merged image plus Hoechst 33342 staining. The punctate accumulation of T β 4 colocalizing with weak TRITC-phalloidin staining represent invadopodia (arrow; see also text). (E) Merged image of a single cell, which clearly shows peripheral areas of T β 4-immunoreactivity co-localizing with TRITC-phalloidin staining (arrowhead) possibly representing focal adhesions. (F) Immunostaining of 3LNLN cells exposed to 2.8 μ M His-T β 4 with anti-His (green) and (F') TRITC-phalloidin after removal of the agarose drop. (F'') Merged image plus Hoechst 33342 staining. Note that most of the cells have become rounded and show intense cytoplasmic and weaker nuclear anti-His staining. Within the nuclei of the rounded cells dots (aggregates) stained strongly by anti-His and weaker by phalloidin are visible. Bars in (C–E) correspond to 20 μ m and in (F) to 50 μ m.

3.6. Effect of Exposure to 2.8 μ M T β 4 and of Overexpressing EGFP-T β 4 on 3LNLN Cells

In order to further analyze the actin cytoskeleton of 3LNLN cells exposed to high His-T β 4, leading to reduction of their migratory activity, we incubated these cells with 2.8 μ M His-T β 4 for 24 h without inclusion into an agarose drop. Subsequently, we performed immunostaining with anti-His (Figure 5A) or anti-T β 4 (Figure 5B–C) and TRITC-phalloidin. The data showed again that most of the cells had a round morphology (Figure 5A), with an almost even distribution of the anti-His immunoreactivity (Figure 5A) and a peripheral concentration of the TRITC-phalloidin stain (Figure 5A'). Occasionally, the anti-T β 4 stain concentrated within the cell nucleus (Figure 5B), whereas the F-actin often appeared irregularly aggregated within the cytoplasm (Figure 5B'). Phase-contrast images showed that these cells had formed bleb-like extensions typical for cells undergoing apoptosis (Figure 5C; see below), which was verified by immunostaining with an anti-active caspase-3 antibody (Figure 5C'). These morphological changes were not observed when 3LNLN cells were exposed to 0.24 μ M T β 4 (see Figure 4C). As the control, we exposed 3LNLN cells to 2.8 μ M His-sc-T β 4 (see sequence comparison in Figure 5B). After 24 h, we did not observe the morphological alterations induced after exposure to 2.8 μ M His-T β 4 (Figure 5D). However, a clear anti-His staining was detected within the cell nuclei (Figure 5D,D'') suggesting that the His-tag itself possessed nuclear localization activity. The fact that both His-T β 4 and His-scT β 4 were both taken up by 3LNLN suggested that their uptake was neither a sequence- nor stereo-specific process.

Plasma membrane blebbing reminiscent of apoptosis was also detected in 3LNLN cells transfected with the pIRES-T β 4-EGFP construct. In 3LNLN presumably overexpressing EGFP-T β 4, we also observed cells rounding and ongoing apoptosis, as shown for a group of cells, some of which strongly expressed EGFP-T β 4 (Figure 5E) and were also positively stained by anti-active caspase-3 (Figure 5E'). Phase-contrast imaging (Figure 5E'') showed the presence of numerous peripheral blebs. Nuclear staining with Hoechst 33342 was merged with EGFP-T β 4 staining (Figure 5E'''), thus strongly supporting the notion that overexpression of T β 4 followed by F-actin disassembly induces cell demise by apoptosis [52].

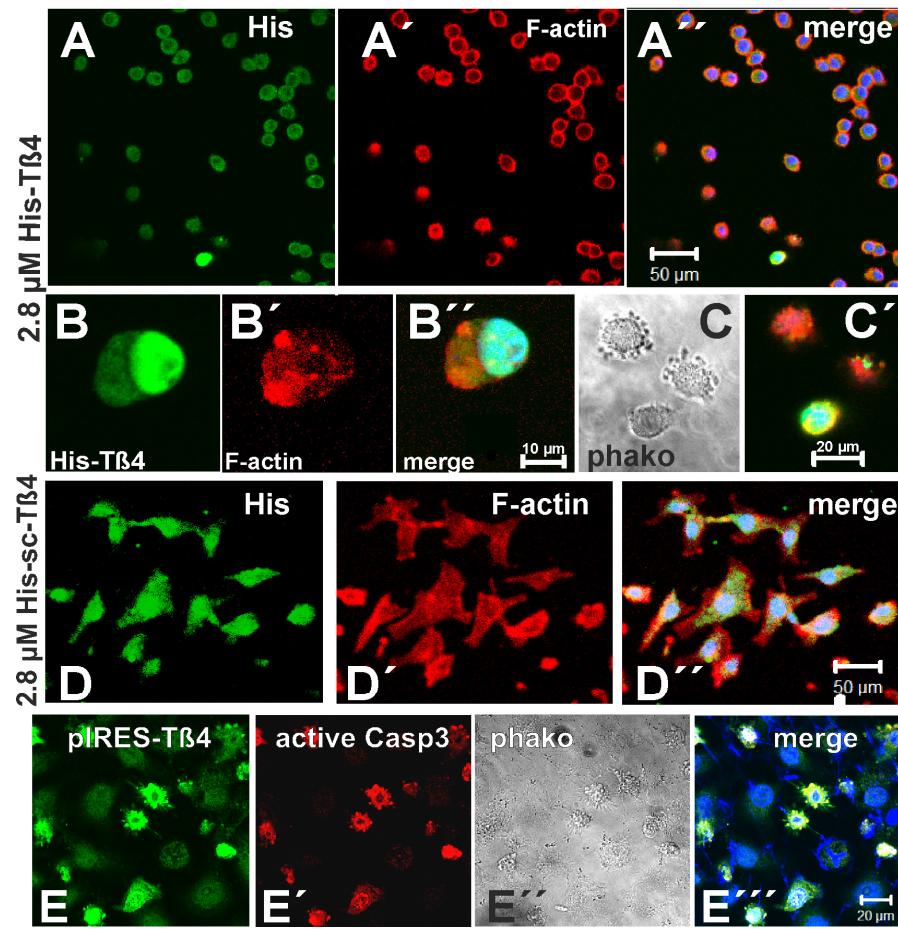


Figure 5. Immunostaining of 3LNLN cells exposed to 2.8 μM His-T β 4 and overexpressing EGFP-T β 4. (A–C) 3LNLN cells exposed to 2.8 μM His-T β 4 (A,B) Immunostaining of 3LNLN cells exposed to 2.8 μM His-T β 4 with anti-His (green) and TRITC-phalloidin. (A) Note that all cells are rounded with a prominent peripheral ring-like staining of anti-His and (A') TRITC-phalloidin. (A'') merged image plus Hoechst 33342 staining. (B) Single cell showing an accumulation of the anti-His immunoreactivity within the nucleus and (B') irregularly aggregated actin within the nucleus but mainly in the cytoplasm. (B'') merged image plus Hoechst 33342 staining. (C) Phase-contrast image of three cells with many peripheral membrane blebs, indicative of apoptosis as characterized by numerous peripheral plasma membrane blebs. (C') Apoptosis was further verified by anti-active caspase-3 staining (green FITC-fluorescence and counterstained with TRITC-phalloidin). (D) 3LNLN cells identically exposed to 2.8 μM His-scrambled-T β 4. Note the absence of cell rounding but prominent anti-His staining of the cell nuclei. (D') TRITC-phalloidin staining suggesting an almost intact-appearing actin cytoskeleton. (D'') merged image plus Hoechst 33342 staining indicating a perinuclear and prominent nuclear anti-His staining. (E) 3LNLN cells transfected with pIRES-T β 4-EGFP vector, leading to overexpression of T β 4. Note that a number of EGFP-T β 4-expressing cells have rounded and formed plasma membrane blebs, as also indicated by phase contrast (E''). These cells are positively stained by anti-active caspase-3 (E'), indicating ongoing apoptosis. (E''') Shows merged image additionally stained by Hoechst 33342, also showing beginning fragmentation of the apoptotic cells into apoptotic bodies containing nuclear fragments (only stained by Hoechst 33342) and weak or absent staining with anti-T β 4 and -active caspase-3 (see (E,E')). Bars correspond to 10 μm (B), 20 μm (C,E), and 50 μm (A,D).

3.7. Co-Localization of T β 4 with ILK in the Presence of Extracellular T β 4

Next, we investigated the intracellular effects of the exposure of the colon tumor cells to 0.24 μM extracellular T β 4 leading to increased migratory activity. This study was prompted by previous data showing that cardiomyocyte progenitor and endothelial cells

internalize extracellular T β 4, which subsequently bound to the LIM-domain containing PINCH protein in complex with ILK and parvin [38]. Indeed, Western blots showed that all the selected tumor cells contain ILK (Figure 6B). ILK localized peripherally, forming focal adhesions (Figure 6C–F), as verified by co-localization of vinculin (Figure 6F) and their association with microfilaments (Figure 6D,E). Supposedly, PINCH together with T β 4 stimulates the kinase activity of ILK by mediating its association to integrins assembled in focal adhesions, into which actin filaments terminate [37,38]. Subsequently, ILK activates the threonine/serine kinases of the AKT family (also known as protein kinases B; PKB) by phosphorylation of AKT-kinases at Ser473 (AKT1) or Ser474 (AKT2), leading to stimulation of cell migration and/or survival by inhibiting apoptosis [53,54].

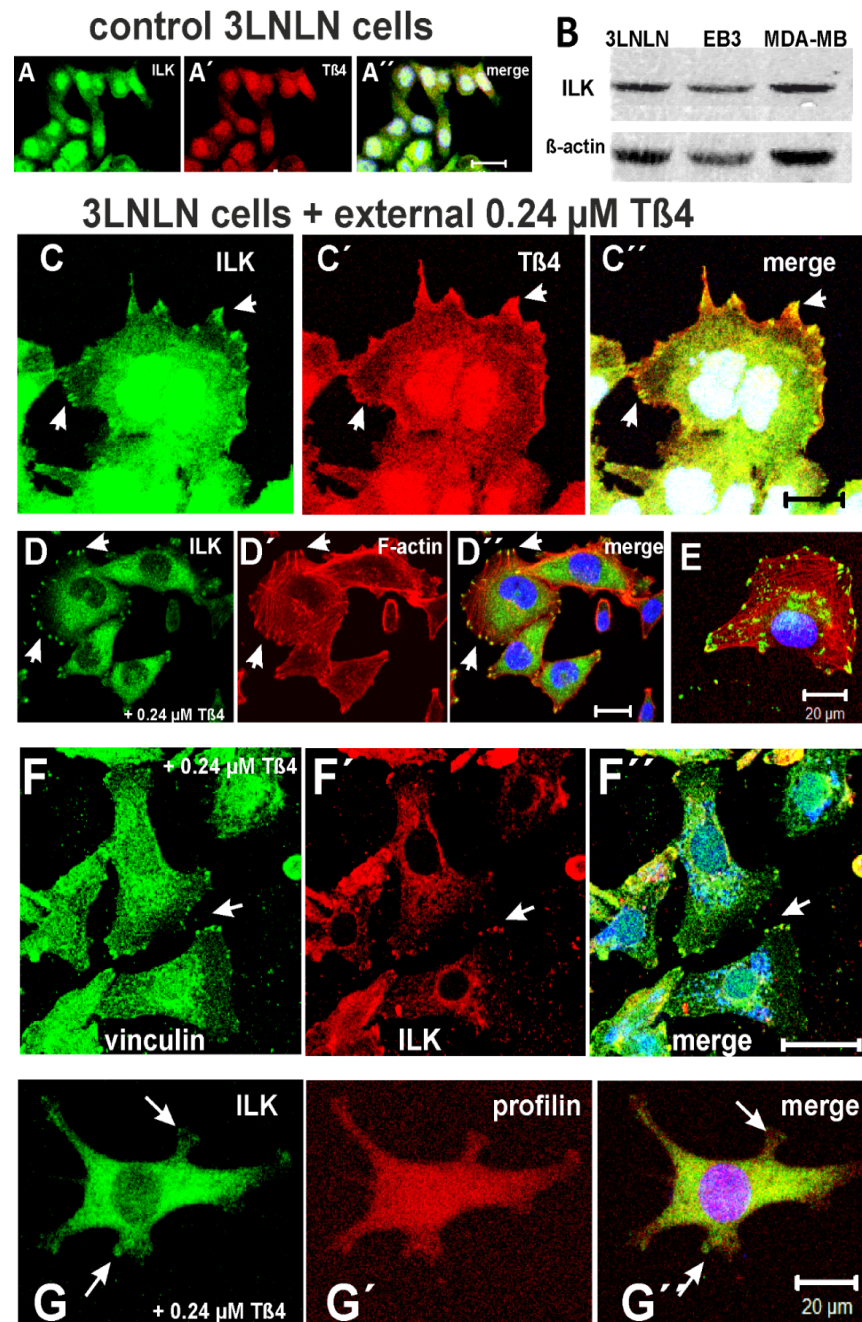


Figure 6. Immunostaining of 3LNLN cells exposed to 0.24 μ M T β 4 with anti-ILK. (A) Control (resting) 3LNLN cells immunostained with anti-ILK and (A') anti-T β 4 (red). (A'') merged image plus Hoechst

33342 staining; note very little peripheral staining of anti-ILK and -T β 4. (B) Western blot of cell homogenates of resting 3LNLN, EB3, and MDA-MB-231 cells (50 μ g protein each), with anti-ILK antibody showing a single band at about 55 kDa and actin at 42 kDa. To demonstrate the monospecificity of the anti-ILK antibody, a complete Western blot is shown in Supplementary Materials Figure S5B. (C) After exposure to 0.24 μ M T β 4 for 24 h the 3LNLN cells were immunostained with anti-ILK and together (C') with anti-T β 4 (red). The arrows in (C–C') point to focal adhesions formed by ILK and co-localizing T β 4. (D,E) ILK immunostaining and (D',E) TRITC-phalloidin staining for F-actin. (D'') merged image plus Hoechst 33342 staining, Arrows point to focal adhesions formed by colocalising ILK and F-actin. (E) Merged image of a single cell clearly showing peripheral focal adhesions and possibly at the plasma membrane underneath the nucleus. (F) Immunostaining with anti-vinculin (green) and (F') anti-ILK (red). (F'') merged image plus Hoechst 33342 staining. Arrow points to focal adhesions. (G) Immunostaining with anti-ILK and (G') anti-profilin. (G'') merged image plus Hoechst 33342 staining indicating possibly weak co-localization of T β 4 and profilin (arrows). For further details see text. All bars correspond to 20 μ m.

Of note, exposure of the additional colon tumor cell lines with 0.24 μ M T β 4 induced only in the more motile SW-480 cell line (see Table S1) the formation of ILK-positive adhesion points with terminating microfilaments, whereas the Caco-2, LS174t, and HT-29 cells maintained their cluster formation (see Figure S6).

In addition, we investigated by immunostaining the localization of profilin in relation to ILK, because previous reports had suggested that T β 4 in complex with actin translocates towards the plasma membrane, where plasma membrane bound profilin might by its higher affinity to actin dissociate the actin:T β 4 complex [38]. The subsequent binding of liberated T β 4 to PINCH of the PINCH-parvin-ILK complex (“PPI-complex”) supposedly activates the phosphokinase activity of ILK [37,38]. We observed by immunostaining with anti-profilin its presence within the cytoplasm of 3LNLN cells and occasionally at the tips of filopodia-like extrusions, where it co-localized with anti-ILK immunoreactivity (Figure 6G). It is however possible that other cytoskeletal components close to the plasma membrane like actin nucleating proteins (Arp2/3 complex or formins) are better suited to separate the actin:T β 4 complex as shown in biochemical assays [26,27]. Furthermore, the formation of a stable ternary profilin:actin:T β 4 complex has been shown suggesting that T β 4 might not necessarily be dissociated from actin by profilin [55].

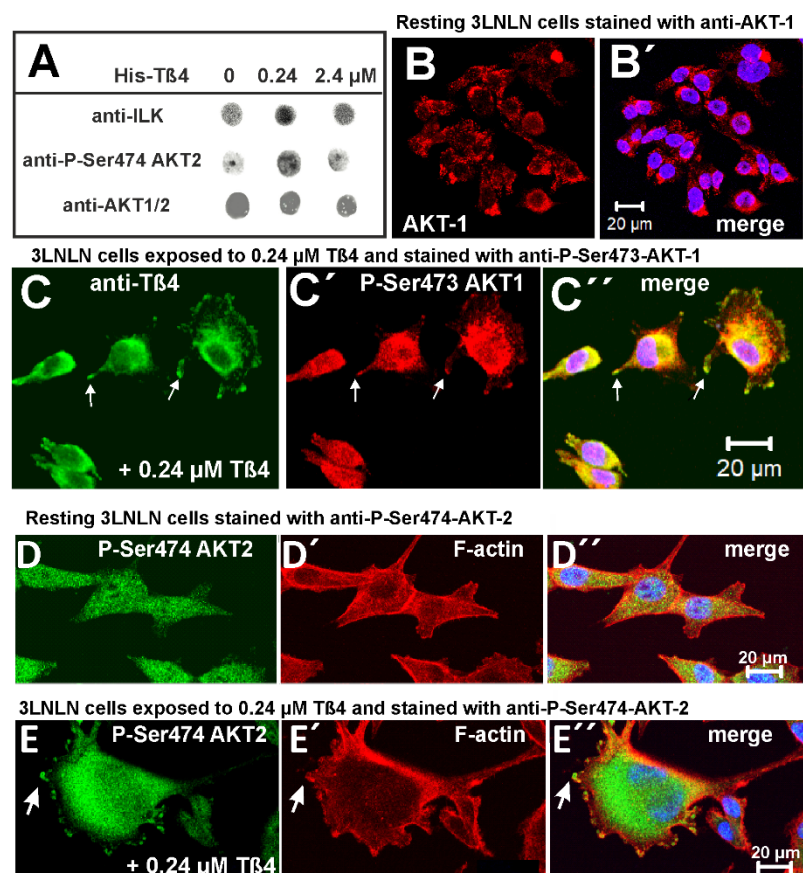
3.8. Extracellular T β 4 Increases the Phosphorylation/Activation of AKT/PKB Proteins

Dot-immunoblots indicated a modulation of the expression of ILK by extracellular T β 4 being high in the presence of 0.24 μ M T β 4 and decreasing at 2.4 μ M T β 4 (Figure 7A, upper row). Using a pan-anti-AKT antibody (recognizing AKT1,2,3) did not indicate a similar response of AKT-proteins to these T β 4 concentrations (Figure 7A, lower row). In contrast, using an antibody against P-Ser474-AKT2 showed a clear increase in phosphorylated AKT2 in homogenates of 3LNLN cells after exposure to 0.24 μ M T β 4 and a decrease at 2.4 μ M T β 4 (Figure 7A, middle row). The quantitative densitometric evaluation of the immunodot experiments is shown in Table 2.

Immunostaining resting 3LNLN cells with anti-pan-AKT indicated a cytoplasmic distribution of AKT proteins (Figure 7B). Immunostaining 3LNLN cells exposed to 0.24 μ M T β 4 with anti-P-Ser473-Akt1 showed an increase in phosphorylated AKT1 and its concentration in peripheral dot-like areas, where it co-localized with T β 4 (Figure 7C).

Table 2. Changes in the relative concentrations of the proteins indicated in cell homogenates of 3LNLN cells before and after exposure to His-T β 4 as determined by dot immunoblotting (see also Figure 8A).

2.4 μ M His-T β 4	0.24 μ M His-T β 4	Control	
107%	141%	100%	anti-ILK
121%	208%	100%	anti-P-Ser474-AKT2
72%	85%	100%	anti-AKT1,2
99%	97%	100%	anti-actin
98%	98%	100%	anti-tubulin

**Figure 7.** Phosphorylation of AKT/PKB by exposure to 0.24 μ M T β 4. (A) Dot blots of cell homogenates of 3LNLN cells before and after exposure for 24 h to 0.24 μ M or 2.4 μ M extracellular T β 4 using the anti-ILK antibody, or antibodies specific for P-Ser473-AKT1 or for P-Ser474-AKT2. The evaluation of the immunodot experiments is given in Table 2. (B) Immunostaining of control (resting) 3LNLN cells with anti-AKT antibody and (B') plus Hoechst 33342 staining. Note the presence of AKT proteins within the cytoplasm. (C) Double immunostaining of 3LNLN cells exposed to 0.24 μ M T β 4 with anti-T β 4 and (C') anti-P-Ser473-AKT1. Note their peripheral co-localization (also indicated by arrows) in (C'') merged image plus Hoechst 33342 staining. (D) Staining of resting 3LNLN cells with anti-P-Ser474-AKT2 and with (D') TRITC-phalloidin. (D'') Merged image plus Hoechst 33342 staining. Note the cytoplasmic dotted anti-P-Ser474-AKT2 staining without prominent co-localization with F-actin. (E) Staining of 3LNLN cells exposed to 2.4 μ M T β 4 with anti-P-Ser474-AKT2 and with (E') TRITC-phalloidin. (E'') Merged image plus Hoechst 33342 staining. Note clear peripheral anti-P-Ser474-AKT2 staining together with prominent co-localization with F-actin possibly forming focal adhesions. All bars correspond to 20 μ m.

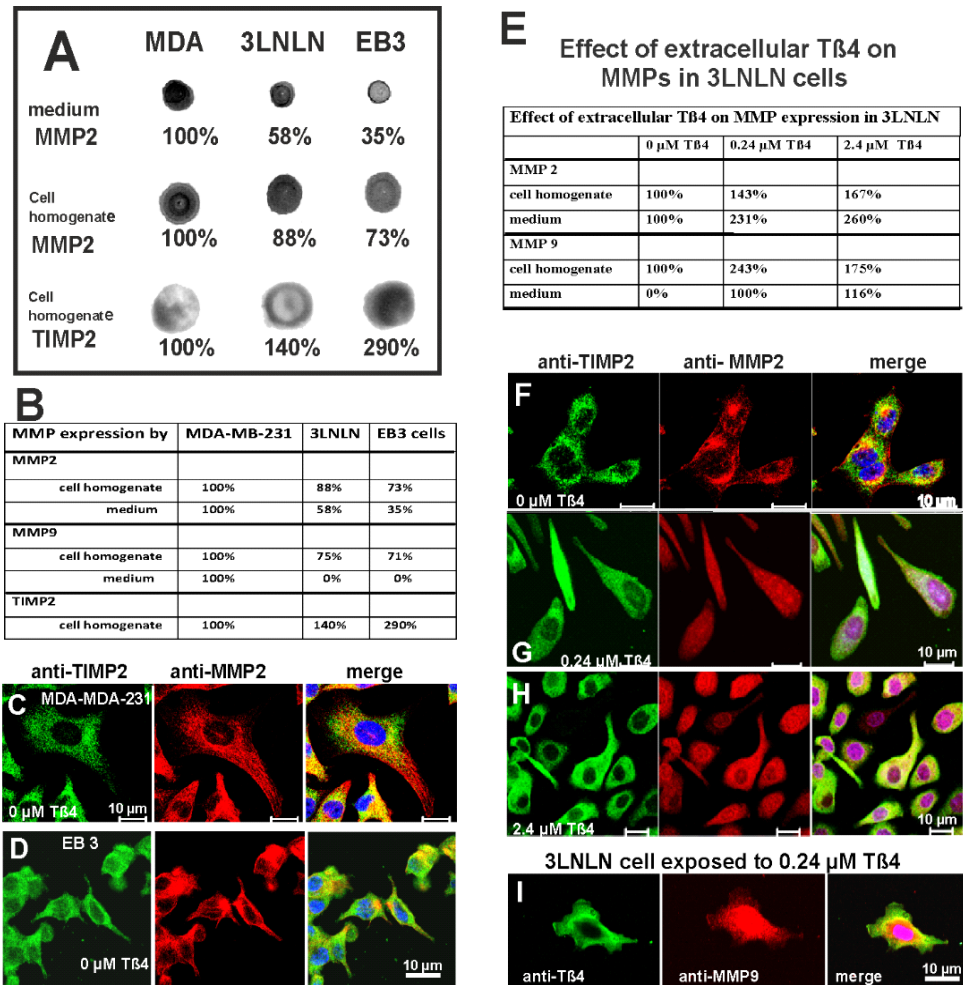


Figure 8. Expression of TIMP2, MMP2 and MMP9 in the different tumor cell lines in the absence of extracellular Tβ4. (A) Dot immunoblots of homogenates and cell medium (50 μg protein/dot) of the three cell lines immunostained with antibodies against MMP2 and TIMP2. To demonstrate the monospecificity of the anti-MMP2 antibody, a complete Western blot is shown in Supplementary Materials Figure S5C depicting an apparent Mr of 65 kDA. (B) Table showing percental evaluation by densitometry (for details, see text). Double immunostaining of (C) MDA-MB-231 and (D) EB3 cells in the absence of extracellular Tβ4 with (C,D) anti-TIMP2 and anti-MMP2. Merged images together with Hoechst 33342 staining (for details, see text). Expression of MMP2, MMP9, and TIMP2 by 3LNLN cells exposed to increasing Tβ4 concentrations. (E) Table of densitometric evaluation of immunodot blots of 3LNLN cell homogenates and respective culture media stained with anti-MMP2 and -MMP9. The values obtained at zero (no exposure to) Tβ4 were set as 100%. Note the intracellular increase in MMP2 and MMP9 expression by exposure to extracellular Tβ4. (F–H) Immunostaining of 3LNLN cells with anti-TIMP2 and -MMP2 after exposure to (F) zero Tβ4, to (G) 0.24 μM Tβ4, and to (H) 2.4 μM Tβ4. Merged images with Hoechst 33342 staining. (I) Immunostaining of 3LNLN cells exposed to 0.24 μM Tβ4 with anti-Tβ4 and -MMP9. Immunostained antigens are indicated at headings above the images. Merged images are plus Hoechst 33342 staining. Bars correspond to 10 μm.

Similar distributions were obtained by staining 3LNLN cells with anti-P-Ser474-Akt2 and TRITC-phalloidin (Figure 7D) when exposed to 0.24 μM Tβ4. These 3LNLN cells showed an increase in P-Ser474-Akt2 immunoreactivity that co-localized with F-actin within presumed adhesion areas (arrows in Figure 7D) and additionally showed a strong cytoplasmic P-Ser474-Akt2 immunoreactivity. Thus, these results support the notion that Tβ4 aided phosphorylation of AKT proteins, also termed phosphokinases B (PKB), by ILK. In contrast, exposure to 2.4 μM Tβ4 led to a decrease in anti-P-Ser474-AKT2 staining but not

to a complete reversal, although migration was inhibited under this condition. Furthermore, peripheral P-Ser474-Akt2-positive contact points were not observed in 3LNLN cells exposed to 2.4 μ M T β 4 (Figure 7E). Table 2 summarizes the immunodot data from 3LNLN cell homogenates, indicating that exposure of 3LNLN and MDA-MB-231 tumor cells to 0.24 μ M extracellular T β 4 leads to a stimulation of the ILK-AKT signaling pathway, in agreement with previous reports that demonstrated, for endothelial and colon tumor cells, Ser474-Akt2 phosphorylation after T β 4 binding to ILK [38,53,54].

Previous data have shown that phosphorylated AKT/PKB proteins (at Ser473 or 474) bind to PIP2 or PIP3 by their pleckstrin-(PH)-domain and thus remain attached to the plasma membrane [56]. Only these membrane-attached AKT/PKB proteins are supposed to possess phosphokinase activity able to phosphorylate target proteins [56]. When, however, released from these phospho-inositols, they become dephosphorylated and inactivated within the cytosol by the PTEN-phosphatase [56]. Only certain AKT-mutants—often with oncogenic potential—are then still active and able to phosphorylate target proteins. The additional cytoplasmic presence of, particularly, P-Ser474-AKT2 might therefore suggest that these tumor cells might contain mutated variants of AKT2.

3.9. Expression of Matrix-Metalloproteinases in Non-Stimulated Carcinoma Cells

Active AKT/PKB-proteins phosphorylate a large number of substrate proteins and thereby lead to increased cell survival (by inhibition of apoptosis) and cell migration also of tumor cells [57]. Tumor cell migration is often supported by expression and secretion of proteases, in particular, of metalloproteinases (MMPs), which degrade extracellular matrix components, especially those forming structural barriers like basement membranes. Indeed, AKT/PKB-proteins activate the transcriptional activity of nuclear factor NF- κ B by phosphorylation of the inhibiting component κ B (I κ B), leading to its subsequent degradation [54]. This process finally induces the expression and secretion of MMPs supporting tumor cell migration [57] and the formation of invadopodia, as observed for 3LNLN cells (see arrows in Figure 4D).

First, we analyzed the expression and secretion of the metalloproteinases MMP2 and MMP9 and the tissue inhibitor of metalloproteinase 2 (TIMP2 [58,59]) by MDA-MB-231, 3LNLN, and EB3 cells before exposure to T β 4. Dot immunoblotting using anti-MMP2 and -TIMP2 showed that, under resting conditions, the three cell lines already expressed MMP2 and TIMP2 (shown in Figure 8A) and MMP9 (see Figure 8B). Both MMPs belong to the gelatinase group and play a crucial role during basement membrane disruption necessary for tumor invasion [59]. Densitometric evaluation of the dot plots (as shown for MMP2 and TIMP2 in Figure 8A) showed the highest MMP2 and MMP9 expression and secretion into the medium by MDA-MB-231 cells (set at 100%; see Figure 8A,B), which also possess the highest migratory activity and invasive potential. Interestingly, the amounts of MMP2 and MMP9 in cell homogenates and the medium increased from EB3 to 3LNLN and MDA-MB-231 cells (Figure 8A,B), i.e., directly correlating with their migratory (invasive) activity, whereby the amounts of MMP2 in cell homogenates and the medium appeared almost equal for the migratory MDA-MB-231 and 3LNLN cells (Figure 8A). Furthermore, we analyzed the expression of TIMP2 (tissue inhibitor of metalloproteinase), which is known to be an effective inhibitor of MMP2 [59]. Anti-TIMP2 reactivity was lowest in MDA-MB-231 cell homogenate (set at 100%) and increased in 3LNLN cells (to 140%) and further in EB3 cells (to 290%), i.e., inversely correlating with their migratory (invasive) activity.

In addition, we performed, in the absence of extracellular T β 4, immunostaining of the three cell lines with anti-MMP2 and -TIMP2 (Figure 8C,D,F). The data showed in all three cell lines the presence of both MMP2 and TIMP2 in granular cytoplasmic structures, which showed no clear co-localization. Indeed, the anti-MPP2 staining indicated in MDA-MB-231

and 3LNLN cells a more peripheral localization of the anti-MMP2 granules, suggesting their transport to possible sites of release into the medium (see also Table B), whereas the granules stained by anti-TIMP2 localized more centrally (Figure 8C,F).

3.10. Exposure to Extracellular T β 4 Increases MMP Expression by the Carcinoma Cells

Next, we investigated by dot immunoblotting whether exposure of 3LNLN cells to 0.24 μ M or 2.4 μ M extracellular T β 4 affected the expression and secretion of metalloproteinases MMP2 and MMP9 (Figure 8F,G–I). Setting the intra- and extracellular amounts of MMP2 and MMP9 of non-exposed cells at 100%, we observed that, after T β 4 exposure, the amounts of intracellular MMP2 and MMP9 increased (Figure 8E). Intracellularly, MMP2 was found highest at 2.4 μ M T β 4, whereas MMP9 was highest at 0.24 μ M T β 4. The extracellular amounts of MMP2 and MMP9 continuously increased with the exposure to 2.4 μ M T β 4, though MMP9 was absent at zero T β 4 (Figure 8E). These data seem to suggest that the expression of MMP2 and MMP9 are differently regulated. However, it is possible that the higher content of MMP2 and MMP9 in the medium was partially due to cell death, as observed after exposure to 2.4 μ M T β 4 (see Figure 5C). Nevertheless, these data indicate that modulating the migratory activity of the 3LNLN cells by different T β 4 concentrations also affects the synthesis and secretion of MMPs.

Finally, we performed immunostaining with antibodies against TIMP2 and MMP2 of 3LNLN cells after their exposure to 0.24 μ M and 2.4 μ M T β 4 (Figure 8G,H). The data obtained suggested an increase in MMP2 in the cytoplasm after exposure to 0.24 μ M extracellular T β 4 (Figure 8G,H), whereas the anti-TIMP2 immunoreactivity appeared unaltered (Figure 8G,H). The immunostaining showed a dotted appearance of TIMP2 and also MMP2 within the cytoplasm, suggesting their presence in secretory vesicles (Figure 8G). In many vesicular structures, both TIMP2 and MMP2 appeared to co-localize; that might not be surprising in view of the fact that TIMP2 is known to activate MMP2 [38,58,59]. After exposure to 2.4 μ M T β 4, the whole cytoplasm of 3LNLN cells was strongly stained by anti-TIMP2 and anti-MMP2 (Figure 8H). Of note, many cells attained a more rounded morphology, as described above (see Figure 7F).

Anti-MMP9 staining of 3LNLN cells exposed to 0.24 μ M T β 4 showed a strong perinuclear staining and a weak punctate cytoplasmic, suggesting their inclusion in secretory vesicles (Figure 8I). The anti-T β 4 staining also showed a strong staining of perinuclear cytoplasm, but also localized prominently underneath the plasma membrane at presumably lamellipodial extensions, possibly supporting actin cycling during locomotion (Figure 8I; see also Figure 4E). Thus, these data seem to indicate that migration and MMP synthesis of these tumor cells respond distinctly to different concentrations of extracellular T β 4.

4. Discussion

The metastasis of cancer cells and the subsequent colonization in distant organs depends on cell intrinsic and extrinsic factors and are the main causes of death of cancer patients. Cancer cells originate by trans-differentiation of epithelial-to-mesenchymal cells (EMTs), which, after reorganization of their actin cytoskeleton, regain motile activity necessary for metastatic invasiveness. However, it has not been possible to define a common trait or genetic signature for the metastatic behavior of cancer cells [1]. Even tumor cells originating from a particular tumor may contain cell subpopulations with differing metastatic activity. The dynamic rearrangements of the actin cytoskeleton, the transient formation of actin-rich membrane extensions, and their attachment to ECM components are essential intrinsic prerequisites for tumor cell metastasis. The dynamic behavior of their actin cytoskeleton is regulated by a multitude of actin-binding proteins (ABPs) and, furthermore, modified by the tumor micro-environment formed by ECM components, cytokines, and

growth factors [1,60]. Here, we investigated under cell culture conditions the effects of cofilin and, in particular, of the actin-binding peptide thymosin β 4 on the migratory behavior of three established cell lines, derived from breast and colorectal cancer, possessing different migratory, i.e., metastatic, potential.

Cofilin is a member of the cofilin/ADF (actin-depolymerizing factor) family and has been shown to stimulate F-actin severing and/or cycling by promoting actin subunit dissociation from the filament minus ends [20,21]. These activities have been shown to be increased in migrating tumor cells [22]. Though the three selected types of tumor cells exhibited different migratory activities, they contained almost equal amounts of cofilin, suggesting that their varying migratory activity was not due to differing cofilin content. Nevertheless, we investigated by transfection experiments the effects of wild-type, constitutively active, or inactive cofilin variants, assuming that differences in cofilin's state of activation might be responsible for the differences in their migratory activity. Our data, however, showed that only transfection with the constitutively active S3A-cofilin mutant led to a slight increase in migratory activity, whereas wild-type and the constitutively inactive S3D-cofilin mutant exerted only a small stimulation or no effect, respectively. These data suggested that, after transfection, de- or phosphorylation of the endogenous cofilin might have reset the concentration of active cofilin.

In contrast, a completely different effect on the migratory activity of the analyzed tumor cells was observed when modulating the intracellular concentration of T β 4 by transfection. The T β 4-shRNA or T β 4-IRES vectors inducing a decrease or increase in intracellular T β 4 led to a clear stimulation or reduction, respectively, of their migratory activity. These results are in agreement with an inverse correlation of their migratory activity and endogenous T β 4 concentrations, as determined by immunoblotting. These data also suggested that the intracellular T β 4 is not regulated by post-translational modifications.

However, it should be mentioned that the HPLC analyses of the intracellular concentrations of β -thymosins showed that these tumor cells contained, in addition to T β 4, also T β 10, a related variant possessing identical actin-sequestering properties [35,36]. T β 10 has been reported to be overexpressed in tumor cells of high malignancy [33,34], though it was also correlated with a high incidence of tumor cell apoptosis [61]. Transfection with the T β 4-shRNA vector might have reduced only the T β 4 isoform, but led to an increase in the migratory activity, probably due to a decrease in total β -thymosin concentration. Conversely, transfection with the pIRES-T β 4 vector led to an overexpression of T β 4 and an increase in the total β -thymosin concentration, leading to F-actin disassembly followed by the inhibition of cell migration. Furthermore, displacement of T β 10 from actin by increased T β 4 might have promoted apoptosis ([61]; see Figure 5).

Transfection experiments usually affect only a small fraction of the targeted cells. Since previous reports had indicated that extracellular T β 4 supports survival of cardiomyocytes [37] and is even taken up by these cells, we exposed the 3LNLN and MDA-MB-231 tumor cells to increasing concentrations of His-tagged T β 4 (varying from zero to 2.8 μ M). The data obtained showed a biphasic response of their migratory activity, with maximal stimulation of migration at 0.24 μ M and inhibition at 2.8 μ M His-T β 4. Immunostaining after His-T β 4 exposure with anti-His demonstrated the intracellular presence of His-T β 4 in all exposed cells, indicating either its passive diffusion or active uptake.

The inhibition of 3LNLN (Figure 5) and MDA-MB-231 (Figure S7) cell migration at high extracellular T β 4 (2.4 to 2.8 μ M) was most probably due to disassembly of their actin filaments, as observed by T β 4 overexpression after T β 4-pIRES transfection. Assuming an intracellular T β 4 concentration of 0.33 μ M in 3LNLN cells before His-T β 4 exposure (see Table 1), it appears possible that at 2.4 to 2.8 μ M extracellular His-T β 4, its intracellular concentration increased high enough to lead to almost complete microfilament disassembly

and thereby to the inhibition of cell migration. Furthermore, we observed cell rounding and, occasionally, an accumulation of anti-His immunoreactivity in the nuclei of rounded cells (see Figure 5B–D). The presence of T β 4 in cell nuclei has been reported previously [62]; however, the presumed accumulation of His-T β 4 in the nuclei and cytoplasm might have led to F-actin depolymerization in both organelles and led to induction of apoptosis [61].

The stimulatory effect up to 0.24 μ M extracellular T β 4 on cell migration appears more difficult to explain, since the stimulating extracellular His-T β 4 concentrations were lower than the intracellular T β 4 (0.33 μ M), except an active uptake of extracellular His-T β 4 occurred, as observed at 2.8 μ M. Indeed, anti-His immunostaining at 0.24 μ M extracellular His-T β 4 showed intracellular anti-His immunoreactivity concentrated at presumed focal adhesion points (see Figure 4C). Alternatively, it has been suggested that T β 4 interacted with a putative receptor protein [63]; however, a beta-thymosin-specific receptor has not yet been identified.

Nevertheless, tumor cell exposure to 0.24 μ M extracellular His-T β 4 appeared to initiate the formation of the ILK-T β 4-PINCH-parvin complex, leading to activation of the integrin-linked kinase (ILK) that activated the ILK-AKT/PKB pathway by phosphorylation of Ser473 of AKT1 and Ser474 of AKT2 (also termed phosphokinases B; PKBs), as demonstrated by immunostaining phospho-specific anti-AKT antibodies. Their phosphorylation is known to lead to increased cell survival by the inhibition of apoptosis, elevated migratory activity, and expression and secretion of matrix metalloproteases (as shown in Figures 7 and 8) further supporting migration.

Thus, our more systematic biological approach shows a concentration-dependent effect of extracellular T β 4 on cell migration and survival and might explain the divergent reports of the effect of increasing T β 4 concentration on tumor cell migration. Immunohistochemical analyses of the biopsy material of colon tumor areas have shown higher T β 4 immunoreactivity of the tumor cells in comparison to non-transformed cells [53]. We assume that those tumor cells correspond to the tumor cells exposed to 0.24 μ M extracellular His-T β 4 in this study.

So far, no reports have provided evidence that in vivo tumor cell migration was stimulated by extracellular T β 4. Furthermore, the serum T β 4 concentration was determined to be only about 0.04 mg/mL (=8 nM) [48], i.e., far below the T β 4 concentration found in this report to stimulate tumor cell migration. However, after blood clotting, T β 4 was found to increase to 16.3 mg/mL (=3.3 μ M) [48], which may be due to T β 4 release from platelets and/or during the formation of extracellular traps (NETs) by neutrophils, which possess also a high content of T β 4 [7,64]. Therefore, it is possible that, under different regimes of chemotherapy, neutrophils are induced to form NETs, increasing the extracellular concentration of T β 4 to a level that supports tumor cell migration. Recent publications have reported contradictory effects of NETs on tumor cell migration (see reviews [65,66]), which might again be due to varying concentrations of the extracellular T β 4 released by different numbers of NET-forming neutrophils. Therefore, more investigations are necessary to elucidate the in vivo “dual” role of the beta-thymosins possibly released by neutrophils. In addition, it might be worth considering the possibility to inhibit tumor cell migration/metastasis by applying T β 4 or its active fragments as a therapeutic measure.

Supplementary Materials: The following supporting information can be downloaded at: <https://www.mdpi.com/article/10.3390/ijtm5020016/s1>. References [67,68] are cited in supplementary file.

Author Contributions: All authors contributed to the study conception and design. A.A.H. performed most of the experiments (cell culture, migration assays, and immunoblotting); K.Ć. and A.J.M. provided the colon carcinoma cell lines and introduced their cultivation conditions; B.B.-S. provided the thymosin beta 4 vectors; E.H. performed the HPLC determination of beta-thymosins in cell homogenates; A.A.H. and H.G.M. devised the study, performed the LSM microscopy, and continuously discussed the results with all authors. The first draft of the manuscript was written by H.G.M., and all authors commented on previous versions of the manuscript. The final and revised manuscript was written by H.G.M. and read, commented on, and approved for submission for publication by all authors. All authors have read and agreed to the published version of the manuscript.

Funding: H.G.M. thanks the Deutsche Forschungsgemeinschaft (Bonn-Bad Godesberg, Germany) for financial support (grant numbers: MA 807/14-2 and MA 807/14-3).

Institutional Review Board Statement: Not applicable.

Informed Consent Statement: Not applicable.

Data Availability Statement: The datasets generated and/or analyzed during the current study are not publicly available, but are available from the corresponding author on reasonable request.

Acknowledgments: We thank Brigitte Jockusch and R. Buchmeier (Braunschweig, Germany) for generating and supplying the monoclonal anti-thymosin β 4 antibody and Saltanat Zhazykbayeva for help with the anti-T β 4 isoform immunodots.

Conflicts of Interest: The authors declare no conflicts of interest.

Abbreviations

ABP	actin-binding protein
ADF	actin-depolymerizing factor
AKT	protein kinase B
ECM	extracellular matrix
EMT	epithelial–mesenchymal transition
F-actin	filamentous actin
FCS	fetal calf serum
FITC	fluorescein isothiocyanate
G-actin	monomeric/globular actin
HEPES	4-(hydroxyethyl)-1-piperazineethanesulfonic acid
ILK	integrin-linked kinase
shRNA	small hairpin RNA
T β 4	thymosin beta4

References

1. Steeg, P.S. Tumor metastasis: Mechanistic insights and clinical challenges. *Nat. Med.* **2006**, *12*, 895–904. [[CrossRef](#)]
2. Friedl, P.; Wolf, K. Plasticity of cell migration: A multiscale tuning model. *J. Cell Biol.* **2010**, *188*, 11–19. [[CrossRef](#)] [[PubMed](#)] [[PubMed Central](#)]
3. Fife, C.M.; McCarroll, J.A.; Kavallaris, M. Movers and shakers: Cell cytoskeleton in cancer metastasis. *Br. J. Pharmacol.* **2013**, *171*, 5507–5523. [[CrossRef](#)]
4. Pollard, T.D.; Cooper, J.A. Actin, a central player in cell shape and movement. *Science* **2009**, *326*, 1208–1212. [[CrossRef](#)] [[PubMed](#)] [[PubMed Central](#)]
5. Schoenenberger, C.A.; Bischler, N.; Fahrenkrog, B.; Aebi, U. Actin's propensity for dynamic filament patterning. *FEBS Lett.* **2002**, *529*, 27–33. [[CrossRef](#)] [[PubMed](#)]
6. Safer, D.; Elzinga, M.; Nachmias, V.T. Thymosin beta 4 and Fx, an actin-sequestering peptide, are indistinguishable. *J. Biol. Chem.* **1991**, *266*, 4029–4032. [[CrossRef](#)] [[PubMed](#)]
7. Cassimeris, L.; Safer, D.; Nachmias, V.T.; Zigmond, S.H. Thymosin beta 4 sequesters the majority of G-actin in resting human polymorphonuclear leukocytes. *J. Cell Biol.* **1992**, *119*, 1261–1270. [[CrossRef](#)] [[PubMed](#)] [[PubMed Central](#)]
8. Mannherz, H.G.; Hannappel, E. The β -thymosins: Intracellular and extracellular activities of a versatile actin binding protein family. *Cell Motil. Cytoskelet.* **2009**, *66*, 839–851. [[CrossRef](#)]

9. Bamberg, J.R. Proteins of the ADF/cofilin family: Essential regulators of actin dynamics. *Annu. Rev. Cell Dev. Biol.* **1999**, *15*, 185–230. [[CrossRef](#)] [[PubMed](#)]
10. Xue, B.; Robinson, R.C. Guardians of the actin monomer. *Eur. J. Cell Biol.* **2013**, *92*, 316–332. [[CrossRef](#)] [[PubMed](#)]
11. Pollard, T.D.; Borisy, G.G. Cellular motility driven by assembly and disassembly of actin filaments. *Cell* **2003**, *112*, 453–465. [[CrossRef](#)]
12. Bravo-Cordero, J.J.; Magalhaes, M.A.; Eddy, R.J.; Hodgson, L.; Condeelis, J. Functions of cofilin in cell locomotion and invasion. *Nat. Rev. Mol. Cell Biol.* **2013**, *14*, 405–415. [[CrossRef](#)]
13. Lai, F.P.L.; Szczodrak, M.; Block, J.; Faix, J.; Breitsprecher, D.; Mannherz, H.G.; Stradal, T.E.B.; Dunn, G.A.; Small, J.V.; Rottner, K. Arp2/3 complex interactions and actin network turnover in lamellipodia. *EMBO J.* **2008**, *27*, 982–992. [[CrossRef](#)]
14. Linder, S.; Cervero, P.; Eddy, R.; Condeelis, J. Mechanisms and roles of podosomes and invadopodia. *Nat. Rev. Mol. Cell Biol.* **2023**, *24*, 86–106. [[CrossRef](#)] [[PubMed](#)]
15. Simiczyjew, A.; Mazur, A.J.; Ampe, C.; Malicka-Błaszczkiewicz, M.; van Troys, M.; Nowak, D. Active invadopodia of mesenchymally migrating cancer cells contain both β and γ cytoplasmic actin isoforms. *Exp. Cell Res.* **2016**, *339*, 206–219. [[CrossRef](#)] [[PubMed](#)]
16. Friedl, P.; Bröcker, E.B. T cell migration in three-dimensional extracellular matrix: Guidance by polarity and sensations. *Dev. Immunol.* **2000**, *7*, 249–266. [[CrossRef](#)] [[PubMed](#)] [[PubMed Central](#)]
17. Wegner, A. Head to tail polymerization of actin. *J. Mol. Biol.* **1976**, *108*, 139–150. [[CrossRef](#)]
18. Carlier, M.F.; Pernier, J.; Montaville, P.; Shekhar, S.; Kühn, S. Control of polarized assembly of actin filaments in cell motility. *Cell. Mol. Life Sci.* **2015**, *72*, 3051–3067. [[CrossRef](#)]
19. dos Remedios, C.G.; Chhabra, D.; Kekic, M.; Dedova, I.V.; Tsubakihara, M.; Berry, D.A.; Nosworthy, N.J. Actin binding proteins: Regulation of cytoskeletal microfilaments. *Physiol. Rev.* **2003**, *83*, 433–473. [[CrossRef](#)] [[PubMed](#)]
20. Carlier, M.F.; Laurent, V.; Santolini, J.; Melki, R.; Didry, D.; Xia, G.-X.; Hong, Y.; Chua, N.-H.; Pantaloni, D. Actin filament depolymerizing factor (ADF/cofilin) enhances the rate of filament turnover: Implication in actin-based motility. *J. Cell Biol.* **1997**, *136*, 1307–1323. [[CrossRef](#)]
21. Andrianantoandro, E.; Pollard, T.D. Mechanism of actin filament turnover by severing and nucleation at different concentrations of ADF/cofilin. *Mol. Cell* **2006**, *24*, 13–23. [[CrossRef](#)] [[PubMed](#)]
22. van Rheenen, J.; Condeelis, J.; Glogauer, M. A common cofilin activity cycle in invasive tumor cells and inflammatory cells. *J. Cell Sci.* **2009**, *122*, 305–311. [[CrossRef](#)] [[PubMed](#)] [[PubMed Central](#)]
23. Tania, N.; Prosk, E.; Condeelis, J.; Edelstein-Keshet, L. A temporal model of cofilin regulation and the early peak of actin barbed ends in invasive tumor cells. *Biophys. J.* **2011**, *100*, 1883–1892. [[CrossRef](#)] [[PubMed](#)] [[PubMed Central](#)]
24. Zarbock, J.; Oschkinat, H.; Hannappel, E.; Kalbacher, H.; Voelter, W.; Holak, T.A. Solution conformation of thymosin beta 4: A nuclear magnetic resonance and simulated annealing study. *Biochemistry* **1990**, *29*, 7814–7821. [[CrossRef](#)] [[PubMed](#)]
25. Irobi, E.; Aguda, A.H.; Larsson, M.; Guerin, C.; Yin, H.L.; Burtnick, L.D.; Blanchoin, L.; Robinson, R.C. Structural basis of actin sequestration by thymosin-beta4: Implications for WH2 proteins. *EMBO J.* **2004**, *23*, 3599–3608. [[CrossRef](#)] [[PubMed](#)] [[PubMed Central](#)]
26. Mannherz, H.G.; Mazur, A.; Jockusch, B.M. Repolymerization of Actin from Actin:Thymosin β 4 complex induced by Diaphanous related formins and Gelsolin. *Ann. N. Y. Acad. Sci.* **2010**, *1194*, 36–43. [[CrossRef](#)]
27. Schönichen, A.; Geyer, M. Fifteen formins for an actin filament: A molecular view on the regulation of human formins. *Biochim. Biophys. Acta.* **2010**, *1803*, 152–163. [[CrossRef](#)] [[PubMed](#)]
28. Al Haj, A.; Mazur, A.J.; Buchmeier, S.; App, C.; Theiss, C.; Silvan, U.; Schoenenberger, C.A.; Jockusch, B.M.; Hannappel, E.; Weeds, A.G.; et al. Thymosin beta4 inhibits ADF/cofilin stimulated F-actin cycling and HeLa cell migration: Reversal by active Arp2/3 complex. *Cytoskeleton* **2014**, *71*, 95–107. [[CrossRef](#)] [[PubMed](#)]
29. Cha, H.J.; Jeong, M.J.; Kleinman, H.K. Role of thymosin beta4 in tumor metastasis and angiogenesis. *J. Natl. Cancer Inst.* **2003**, *95*, 1674–1680. [[CrossRef](#)]
30. Yamamoto, T.; Gotoh, M.; Kitajima, M.; Hirohashi, S. Thymosin beta-4 expression is correlated with metastatic capacity of colorectal carcinomas. *Biochem. Biophys. Res. Commun.* **1993**, *193*, 706–710. [[CrossRef](#)] [[PubMed](#)]
31. Ricci-Vitiani, L.; Mollinari, C.; di Martino, S.; Biffoni, M.; Pilozi, E.; Pagliuca, A.; de Stefano, M.C.; Circo, R.; Merlo, D.; De Maria, R.; et al. Thymosin beta4 targeting impairs activity of colon cancer stem cells. *FASEB J.* **2010**, *24*, 4291–4301. [[CrossRef](#)] [[PubMed](#)]
32. Popow-Wozniak, A.; Mazur, A.J.; Mannherz, H.G.; Malicka-Błaszczkiewicz, M.; Nowak, D. Cofilin overexpression affects actin cytoskeleton organization and migration of human colon adenocarcinoma cells. *Histochem. Cell Biol.* **2012**, *138*, 725–736. [[CrossRef](#)] [[PubMed](#)]
33. Califano, D.; Monaco, C.; Santelli, G.; Giuliano, A.; Veronese, M.L.; Berlingieri, M.T.; de Franciscis, V.; Berger, N.; Trapasso, F.; Santoro, M.; et al. Thymosin beta-10 gene overexpression correlated with the highly malignant neoplastic phenotype of transformed thyroid cells in vivo and in vitro. *Cancer Res.* **1998**, *58*, 823–828. [[PubMed](#)]
34. Wang, B.; Wang, Z.; Zhang, T.; Yang, G. Overexpression of thymosin β 10 correlates with disease progression and poor prognosis in bladder cancer. *Exp. Ther. Med.* **2019**, *18*, 3759–3766. [[CrossRef](#)] [[PubMed](#)] [[PubMed Central](#)]

35. Yu, F.X.; Lin, S.C.; Morrison-Bogorad, M.; Atkinson, M.A.; Yin, H.L. Thymosin beta 10 and thymosin beta 4 are both actin monomer sequestering proteins. *J. Biol. Chem.* **1993**, *268*, 502–509. [[CrossRef](#)] [[PubMed](#)]
36. Yu, F.X.; Lin, S.C.; Morrison-Bogorad, M.; Yin, H.L. Effects of thymosin beta 4 and thymosin beta 10 on actin structures in living cells. *Cell Motil. Cytoskelet.* **1994**, *27*, 13–25. [[CrossRef](#)] [[PubMed](#)]
37. Bock-Marquette, I.; Saxena, A.; White, M.D.; Dimaio, J.M.; Srivastava, D. Thymosin beta4 activates integrin-linked kinase and promotes cardiac cell migration, survival and cardiac repair. *Nature* **2004**, *432*, 466–472. [[CrossRef](#)]
38. Fan, Y.; Gong, Y.; Ghosh, P.K.; Graham, L.M.; Fox, P.L. Spatial coordination of actin polymerization and ILK-Akt2 activity during endothelial cell migration. *Dev. Cell.* **2009**, *16*, 661–674. [[CrossRef](#)] [[PubMed](#)] [[PubMed Central](#)]
39. Niland, S.; Riscanevo, A.X.; Eble, J.A. Matrix metalloproteinases shape the tumor microenvironment in cancer progression. *Int. J. Mol. Sci.* **2021**, *23*, 146. [[CrossRef](#)] [[PubMed](#)] [[PubMed Central](#)]
40. Mannherz, H.G.; Gonsior, S.M.; Gremm, D.; Wu, X.; Pope, B.J.; Weeds, A.G. Activated cofilin colocalizes with Arp2/3 complex in apoptotic blebs during programmed cell death. *Eur. J. Cell Biol.* **2005**, *84*, 503–515. [[CrossRef](#)]
41. Wirsching, H.-G.; Kretz, O.; Morosan-Puopolo, G.; Chernogorova, P.; Theiss, C.; Brand-Saberi, B. Thymosin β 4 induces folding of the developing optic tectum in the chicken (*Gallus domesticus*). *J. Comp. Neurol.* **2011**, *520*, 1650–1662. [[CrossRef](#)] [[PubMed](#)]
42. Dai, F.; Yusuf, F.; Farjah, G.H.; Brand-Saberi, B. RNAi-induced targeted silencing of developmental control genes during chicken embryogenesis. *Dev. Biol.* **2005**, *285*, 80–90. [[CrossRef](#)] [[PubMed](#)]
43. Nowak, D.; Krawczenko, A.; Duoe, D.; Malicka-Blaszkiewicz, M. Actin in human colonadenocarcinoma cells with different metastatic potential. *Acta Biochim Pol.* **2002**, *49*, 823–828. [[CrossRef](#)]
44. Harrington, J.T., Jr.; Stastny, P. Macrophage migration from an agarose droplet: Development of a micromethod for assay of delayed hypersensitivity. *J. Immunol.* **1973**, *110*, 752–759. [[CrossRef](#)] [[PubMed](#)]
45. Low, T.L.; Lin, C.Y.; Pan, T.L.; Chiou, A.J.; Tsugita, A. Structure and immunological properties of thymosin beta 9 Met, a new analog of thymosin beta 4 isolated from porcine thymus. *Int. J. Pept. Protein Res.* **1990**, *36*, 481–488. [[CrossRef](#)] [[PubMed](#)]
46. Röder, B. Biochemische Und Zellbiologische Untersuchungen Des Intrinsisch Unstrukturierten Proteins Thymosin Beta 4. Ph.D. Thesis, Ruhr-University, Bochum, Germany, 2012.
47. Bradford, M.M. A rapid and sensitive method for the quantitation of microgram quantities of protein utilizing the principle of protein-dye binding. *Anal. Biochem.* **1976**, *72*, 248–254. [[CrossRef](#)] [[PubMed](#)]
48. Hannappel, E.; van Kampen, M. Determination of thymosin beta 4 in human blood cells and serum. *J. Chromatogr.* **1987**, *397*, 279–285. [[CrossRef](#)] [[PubMed](#)]
49. Hermoso, M.; Olivero, P.; Torres, R.; Riveros, A.; Quest, A.F.; Stutzin, A. Cell volume regulation in response to hypotonicity is impaired in HeLa cells expressing a protein kinase-C alpha mutant lacking kinase activity. *J. Biol. Chem.* **2004**, *279*, 17681–17689. [[CrossRef](#)] [[PubMed](#)]
50. Bamburg, J.R.; Bernstein, B.W. Roles of ADF/cofilin in actin polymerization and beyond. *F1000 Biol. Rep.* **2010**, *2*, 62. [[CrossRef](#)] [[PubMed](#)] [[PubMed Central](#)]
51. Low, T.L.; Goldstein, A.L. Thymosins: Structure, function and therapeutic applications. *Thymus* **1984**, *6*, 27–42. [[PubMed](#)]
52. Aoki, K.; Sato, S.; Harada, S.; Uchida, S.; Iwasa, Y.; Ikenouchi, J. Coordinated changes in cell membrane and cytoplasm during maturation of apoptotic bleb. *Mol. Biol. Cell.* **2020**, *31*, 833–844. [[CrossRef](#)] [[PubMed](#)] [[PubMed Central](#)]
53. Piao, Z.; Hong, C.S.; Jung, M.R.; Choi, C.; Park, Y.K. Thymosin β 4 induces invasion and migration of human colorectal cancer cells through the ILK/AKT/ β -catenin signaling pathway. *Biochem. Biophys. Res. Commun.* **2014**, *452*, 858–864. [[CrossRef](#)] [[PubMed](#)]
54. Bai, D.; Ueno, L.; Vogt, P.K. Akt-mediated regulation of NF κ B and the essentialness of NF- κ B for the oncogenicity of PI3K and Akt. *Int. J. Cancer* **2009**, *125*, 2863–2870. [[CrossRef](#)] [[PubMed](#)] [[PubMed Central](#)]
55. Yarmola, E.G.; Parikh, S.; Bubb, M.R. Formation and implications of a ternary complex of profilin, thymosin beta 4, and actin. *J. Biol. Chem.* **2001**, *276*, 45555–45563. [[CrossRef](#)] [[PubMed](#)]
56. Ebner, M.; Lučić, I.; Leonard, T.A.; Yudushkin, I. PI(3,4,5)P₃ Engagement Restricts Akt Activity to Cellular Membranes. *Mol Cell.* **2017**, *65*, 416–431.e6. [[CrossRef](#)] [[PubMed](#)]
57. Kim, D.; Kim, S.; Koh, H.; Yoon, S.O.; Chung, A.S.; Cho, K.S.; Chung, J. Akt/PKB promotes cancer cell invasion via increased motility and metalloproteinase production. *FASEB J.* **2001**, *11*, 1953–1962. [[CrossRef](#)] [[PubMed](#)]
58. Hey, S.; Linder, S. Matrix metalloproteinases at a glance. *J. Cell Sci.* **2024**, *137*, jcs261898. [[CrossRef](#)] [[PubMed](#)]
59. Raezadeh-Sarmazdeh, M.; Do, L.D.; Hritz, B.G. Metalloproteinases and Their Inhibitors: Potential for the Development of New Therapeutics. *Cells* **2020**, *9*, 1313. [[CrossRef](#)] [[PubMed](#)] [[PubMed Central](#)]
60. Lambert, A.W.; Zhang, Y.; Weinberg, R.A. Cell-intrinsic and microenvironmental determinants of metastatic colonization. *Nat. Cell Biol.* **2024**, *26*, 687–697. [[CrossRef](#)]
61. Hall, A.K. Thymosin beta-10 accelerates apoptosis. *Cell Mol. Biol. Res.* **1995**, *41*, 167–180. [[PubMed](#)]
62. Huff, T.; Rosorius, O.; Otto, A.M.; Müller, C.S.; Ballweber, E.; Hannappel, E.; Mannherz, H.G. Nuclear localization of the G-actin sequestering peptide thymosin beta4. *J. Cell Sci.* **2004**, *117*, 5333–5341. [[CrossRef](#)] [[PubMed](#)]

63. Renault, L. Intrinsic, Functional, and Structural Properties of β -Thymosins and β -Thymosin/WH2 Domains in the Regulation and Coordination of Actin Self-Assembly Dynamics and Cytoskeleton Remodeling. *Vitam. Horm.* **2016**, *102*, 25–54. [[PubMed](#)]
64. Mannherz, H.G.; Budde, H.; Jarkas, M.; Hassoun, R.; Malek-Chudzik, N.; Mazur, A.J.; Skuljec, J.; Pul, R.; Napirei, M.; Hamdani, N. Reorganization of the actin cytoskeleton during the formation of neutrophil extracellular traps (NETs). *Eur. J. Cell Biol.* **2024**, *103*, 151407. [[CrossRef](#)] [[PubMed](#)]
65. Khan, U.; Chowdhury, S.; Billah, M.M.; Islam, K.M.D.; Thorlacius, H.; Rahman, M. Neutrophil Extracellular Traps in Colorectal Cancer Progression and Metastasis. *Int. J. Mol. Sci.* **2021**, *22*, 7260. [[CrossRef](#)] [[PubMed](#)] [[PubMed Central](#)]
66. Mousset, A.; Bellone, L.; Gaggioli, C.; Albregues, J. NETscape or NEThance: Tailoring anti-cancer therapy. *Trends Cancer* **2024**, *10*, 655–667. [[CrossRef](#)] [[PubMed](#)]
67. Huff, T.; Müller, C.S.; Otto, A.M.; Netzker, R.; Hannappel, E. β -Thymosins, small acidic peptides with multiple functions. *Int. J. Biochem. Cell Biol.* **2001**, *33*, 205–220. [[CrossRef](#)]
68. Pope, B.J.; Gonsior, S.M.; Yeoh, S.; McGough, A.; Weeds, A.G. Uncoupling actin filament fragmentation by cofilin from increased subunit turnover. *J. Mol. Biol.* **2000**, *298*, 649–661. [[CrossRef](#)]

Disclaimer/Publisher's Note: The statements, opinions and data contained in all publications are solely those of the individual author(s) and contributor(s) and not of MDPI and/or the editor(s). MDPI and/or the editor(s) disclaim responsibility for any injury to people or property resulting from any ideas, methods, instructions or products referred to in the content.